

Glucocorticoid Receptor-Binding and Transcriptome Signature in Cardiomyocytes

Elena Severinova, PhD;* Saleena Alikunju, PhD;* Wei Deng, MD, PhD;† Puneet Dhawan, PhD; Nazish Sayed, MD, PhD; Danish Sayed, MD, PhD

Background—An increase in serum cortisol has been identified as a risk factor for cardiac failure, which highlights the impact of glucocorticoid signaling in cardiomyocytes and its influence in the progression of failure. Dexamethasone, a synthetic glucocorticoid, is sufficient for induction of cardiomyocyte hypertrophy, but little is known of the glucocorticoid receptor (GR) genome-binding and -dependent transcriptional changes that mediate this phenotype.

Methods and Results—In this study using high-resolution sequencing, we identified genomic targets of GR and associated change in the transcriptome after 1 and 24 hours of dexamethasone treatment. We showed that GR associates with 6482 genes in the cardiac genome, with differential regulation of 738 genes. Interestingly, alignment of the chromatin immunoprecipitation and RNA sequencing data show that, after 1 hour, 69% of differentially regulated genes are associated with GR and identify as regulators of RNA pol II-dependent transcription. Conversely, after 24 hours only 45% of regulated genes are associated with GR and involved in dilated and hypertrophic cardiomyopathies as well as other growth-related pathways. In addition, our data also reveal that a majority of genes (76.42%) associated with GR show incremental changes in transcript abundance and are genes involved in basic cellular processes that might be regulated by the dynamics of promoter-paused RNA pol II, as seen in hearts undergoing hypertrophy. In vivo administration of dexamethasone resulted in similar changes in the cardiac transcriptome, as seen in isolated cardiomyocytes.

Conclusions—Our data reveal genome-wide GR binding sites in cardiomyocytes, identify novel targets and GR-dependent change in the transcriptome that induces and contributes to cardiomyocyte hypertrophy. (*J Am Heart Assoc.* 2019;8:e011484. DOI: 10.1161/JAHA.118.011484.)

Key Words: dexamethasone • gene expression/regulation • gene transcription • genome-wide analysis • glucocorticoid receptor • glucocorticoid receptor-dependent transcription • hypertrophic transcriptome • hypertrophy

Glucocorticoids (Gc) and mineralocorticoids, classified as corticosteroids, are secreted from the adrenal cortex and play a vital role in many physiological processes including

organogenesis, fluid balance, and responses to cellular stress. They have also been implicated in many pathophysiological conditions, including cardiovascular disease states such as hypertension and cardiac failure.^{1,2} Nuclear receptor subfamily 3, group C, member 1 and nuclear receptor subfamily 3, group C, member 2 code for the glucocorticoid receptor (GR) and mineralocorticoid receptor, respectively.³ Activation of these cytoplasmic receptors by binding of respective ligands results in their nuclear translocation, where they function as transcription factors by binding to the genome and mediating changes in gene expression. Cytoplasmic GR is associated with a chaperone complex that includes HSP90, HSP70, and several cochaperones, which control GR translocation and abundance, thus regulating its function.⁴⁻⁶

The mineralocorticoid receptor has an affinity to bind to both Gc and mineralocorticoids, whereas GR has a high affinity for Gc. Interestingly, due to domain similarities, mineralocorticoid receptor and GR have been shown to exhibit common genomic binding sites, albeit with different downstream effects with respect to transcriptomes and functions.⁷ There is consistency between the role of

From the Department of Cell Biology and Molecular Medicine (E.S., S.A., W.D., D.S.), and Genomics Center, Department of Microbiology Biochemistry and Molecular Genetics (P.D.), Rutgers New Jersey Medical School, Newark, NJ; Cardiovascular Institute, Stanford University, Stanford, CA (N.S.).

Accompanying Figures S1 through S9 and Tables S1 through S3 are available at <https://www.ahajournals.org/doi/suppl/10.1161/JAHA.118.011484>

*Dr Severinova and Dr Alikunju contributed equally to this work.

†Dr Wei Deng is currently located at the Department of Bioelectric Medicine, Northwell Health, Manhasset, NY.

Correspondence to: Danish Sayed, MD, PhD, Department of Cell Biology and Molecular Medicine, Rutgers New Jersey Medical School, 185 South Orange Avenue, Medical Science Building, G-653, Newark, NJ 07103. E-mail: sayeddh@njms.rutgers.edu

Received November 9, 2018; accepted February 12, 2019.

© 2019 The Authors. Published on behalf of the American Heart Association, Inc., by Wiley. This is an open access article under the terms of the Creative Commons Attribution-NonCommercial-NoDerivs License, which permits use and distribution in any medium, provided the original work is properly cited, the use is non-commercial and no modifications or adaptations are made.

Clinical Perspective

What Is New?

- In this study we identify and present a comprehensive genome-wide occupancy status of activated glucocorticoid receptor and glucocorticoid-dependent change in transcriptome at an early and a late time point that contributes to the hypertrophic phenotype in cardiomyocytes.
- We show that early direct targets of glucocorticoid receptor include mostly transcriptional regulators followed by genes that are involved in development of cardiomyopathies and other growth-related pathways.
- Ingenuity pathway analysis lists cardiac hypertrophy and failure at the top of a toxicity list for genes dysregulated after 24 hours of dexamethasone treatment.

What Are the Clinical Implications?

- Dexamethasone, a synthetic glucocorticoid, is frequently used in clinics for its potent anti-inflammatory effects, both locally and systemically.
- In vivo data in mice injected with dexamethasone for 1 or 24 hours show similar transcriptional changes in direct targets of the glucocorticoid receptor, as seen in isolated cardiomyocytes treated with dexamethasone.
- Therefore, understanding the downstream effects of dexamethasone is essential to understand its influence on heart, especially in cases with preexisting cardiac ailments.

mineralocorticoid receptors in the heart and their effects under cardiac stress conditions; however, the effects of GR activation in cardiomyocytes have been conflicting and require detailed systematic examination, especially because circulating serum Gc has been associated with increased mortality in patients with heart failure.^{8,9}

GR is highly expressed in cardiomyocytes and has both genomic and nongenomic effects. Dexamethasone (dex)-mediated activation of GR results in an increase in cardiomyocyte size, suggesting that GR activation is sufficient for cardiomyocyte hypertrophy, which is further exaggerated in the presence of growth stimulation.¹⁰ Interestingly, although studies have shown this phenotype in isolated myocytes,¹¹⁻¹³ mice with cardiac-specific knockdown of GR also presented with a similar phenotype of hypertrophy and cardiac failure as early as 3 months of age.¹⁴ GR function is essential for heart development, where GR activation is associated with cardiomyocyte differentiation in fetal and neonatal cardiomyocytes.¹⁵⁻¹⁸ GRs also modulate cardiac metabolism¹⁹⁻²¹ and have been shown to alter calcium signaling in cardiomyocytes, contributing to cardiac remodeling and dysfunction.^{22,23} Nongenomic effects of the GR have been attributed to its localization to cell membrane and mitochondria after Gc-GR binding,²⁴ which may be working in coordination with the genomic targets to mediate

downstream function and contributing to the hypertrophic phenotype. These studies highlight the importance and the critical balance of GR signaling in cardiac myocytes and its function as an inducer of hypertrophy and failure versus its role in restraining cardiac fibrosis and preventing cardiac failure.

In this study we examined the GR signaling in cardiac myocytes in a systematic and detailed whole-genome approach, which led to identification of the novel direct and secondary targets of GR in cardiac myocytes. Here, we present the GR-dependent changes in the cardiomyocyte transcriptome that play a role in development of the observed hypertrophic phenotype.

Materials and Methods

We have provided all the supporting data and results in this article and online supplementary files.

Neonatal Myocyte Culture and Treatments

Neonatal myocytes were cultured as previously described.²⁵ Briefly, hearts from 1-day-old Sprague-Dawley rats were isolated and dissociated. Enrichment of cardiac myocytes was performed using a Percoll gradient followed by differential preplating to eliminate any contaminating nonmyocytes. Cells were plated in DMEM-F12 (high glucose with L-glutamine and HEPES) with 10% fetal bovine serum for 24 hours, at which time the medium was changed to serum-free medium. Cultured cardiomyocytes were treated with ethanol 100% (diluent control) or dexamethasone (D1756, Sigma, St. Louis, MO) 100 nmol/L for additional time periods of 1 hour, 6 hours or 24 hours, as indicated. The isolation of primary cardiomyocyte was approved by the Institutional Animal Care and Use Committee at Rutgers, The State University of New Jersey. Female Sprague-Dawley rats with 1-day-old litters (male and female) were purchased from Envigo Inc, Princeton, NJ.

ChIP-Seq

Neonatal cardiac myocytes cultured from 40 hearts isolated from 1-day-old Sprague-Dawley rat pups were treated with ethanol (control) or dexamethasone (100 nmol/L) for 1 hour; cells were fixed, collected, and sent to Active Motif (Carlsbad, CA) for GR chromatin immunoprecipitation sequencing (ChIP-Seq). GR ChIP-Seq was performed using anti-GR antibody (sc-8992, Santa Cruz Biotechnology, Dallas, TX) on 25 µg of chromatin from control, dex-treated, and input samples by Illumina (San Diego, CA) NextSeq 500 sequencing.

ChIP-Seq Data Analysis

Bioinformatics on the sequencing data generated was performed by Active Motif, Inc, as described previously.^{26,27}

The data explanation from Active Motif includes the following: *Sequence analysis*: A 75-nt sequence generated by sequencing reads was mapped to the rn5 genome using the BWA algorithm, and the information was stored in BAM format. Only reads that aligned with no more than 2 mismatches and mapped uniquely were used in the analysis. *Determination of Fragment Density*: Aligned reads (tags) were extended in silico at their 3' ends to a length of 150 to 250 bp. To identify the density of fragments along the genome, the genome was divided into 32-nt bins, and the number of fragments in each bin was determined, stored in a bigwig file, and visualized on genome browsers. *Peak Finding*: Genomic regions with enrichments in tag numbers were termed “intervals” and defined by the chromosome number and start and end coordinates. Then 13 366 963 normalized tags were used for peak calling using a MACS 2.1.0 algorithm²⁸ with default cutoff *P* value 10^{-7} for narrow peaks and 0.1 for broad peaks. The MACS method was suitable for identifying binding sites of transcription factors with discrete binding sites such as consensus sequence or histone marks. The MACS method looked for significant enrichments in the ChIP-IP data file when compared with the input data file. Peak filtering was performed by removing false ChIP-Seq peaks as defined within the ENCODE blacklist. *Active regions*: To compare peak metrics between 2 samples, overlapping intervals were grouped into “active regions,” defined by the start coordinate of the most upstream interval and the end coordinate of the most downstream interval. In locations where only 1 sample had an interval, that interval defined the active region. *Annotations*: Intervals, active regions, their genomic locations along with proximities to gene annotations, and other genomic features were determined and presented in an Excel spreadsheet. Average and peak fragment densities within intervals and active regions were compiled. Data obtained were sorted based on the ratio of dex versus control, and subsets were made for manuscript preparation with proper data representation and presentation.

RNA Sequencing

Neonatal cardiac myocytes cultured similarly to those for ChIP-Seq were treated with ethanol (control) or dexamethasone (100 nmol/L) for 1 or 24 hours. RNA sequencing (RNAseq) was performed independently on RNA obtained from 2 cultures and presented as their average. Cells were sent to Active Motif for RNA isolation and RNAseq, followed by bioinformatics, which included data analysis and integration with GR ChIP-Seq data. Directional poly-A RNAseq libraries were prepared and sequenced as P75 (75-bp paired-end reads) on Illumina NextSeq 500 to a depth of 47 to 53 mol/L read pairs. The “TopHat” algorithm was used to

align the reads to the rn5 genome. The alignments in the BAM files were further analyzed using the Cufflinks suite of programs. Cufflinks was run using the rn5 genes as reference database, and output shows the known genes with their RNAseq metrics (as fragments per kilobase of exon model per million mapped fragments), but novel transcripts were not identified. RNA from 2 independent cultures (n=2) were analyzed as 3×2 replicate samples generating 6 Cufflinks outputs, which were compared using Cuffdiff. All these files were opened and converted to Excel (Microsoft, Redmond, WA) tables. The Excel tables include *q*- and *P* values, and by default, genes with *q*-values <0.05 were designated as significant. RNAseq data were verified by quantitative polymerase chain reaction (qPCR) for mRNA abundance of selected genes. The data were further integrated with the GR ChIP-Seq using active regions, which were sorted based on log₂-fold change (Log₂FC) for categorization and analysis. Heatmap for the differentially regulated genes was generated using Heatmapper,²⁹ with complete linkage for clustering and Euclidean distance measurement method. Box plots and Log₂FC graphs were generated using Prism 7, and qPCR data were graphed using Microsoft Excel.

Genome Browsers

Integrated Genomic Viewer³⁰ was used for visualization of integrated GR ChIP-Seq and RNAseq data.

Gene Expression Omnibus Submissions

GR ChIP-Seq and RNAseq data have been uploaded to NCBI Gene Expression Omnibus with series GSE114767, which is a superseries of GSE116616 (ChIP-Seq data) and GE114766 (RNAseq data). RNA pol II ChIP-Seq data are available on Gene Expression Omnibus with series GSE50637.

ChIP Quantitative PCR

Cultured rat neonatal cardiomyocytes were treated with ethanol or dexamethasone (100 nmol/L) for 1 or 24 hours. The cells were fixed and collected as described previously.²⁶ ChIP was performed using anti-pol II antibody (ab5095) or IgG (antirabbit) following Abcam (Cambridge, UK) ChIP protocol X-ChIP. Sonication to shear DNA was performed using an S2 Covaris (Woburn, MA) sonicator. Quantitative PCR was performed on immunoprecipitated DNA fragments using primer-probe sets ordered from Integrated DNA Technologies (Coralville, IA) encompassing the transcription start site of *Trapp6b* and *Mapk1* specific to rat genome.

Immunocytochemistry

Cells were fixed as described previously.³¹ Cells were stained using anti-GR (3660S, Cell Signaling Technology, Danvers, MA) and antiactinin (A7732, Sigma, St. Louis, MO). Prolong gold (Invitrogen, Carlsbad, CA) used for mounting contains DAPI for nuclear staining. Image J³² was used for cell surface area measurements for isolated cardiomyocytes.

Western Blotting

Cardiomyocytes were fractionated using a subcellular protein fractionation kit for cultured cells (Thermo Fisher, Waltham, MA; cat # 78840) per the manufacturer-provided protocol. Lysate was separated on gradient (4% to 12%) XT gels (Bio-Rad, Hercules, CA) and probed for anti-GR (3660S, Cell Signaling), anti-GAPDH (97166S, Cell Signaling), and anti-H2b (12364S, Cell Signaling).

Quantitative PCR

Total RNA was isolated from cardiomyocytes after the indicated treatments and was reverse-transcribed to cDNA using a High-Capacity cDNA Reverse Transcription Kit (Thermo Fisher), as advised in manufacturer's protocol. The cDNA was used for qPCR with an Applied Biosystems 7500 thermocycler using Taqman gene expression assays (a complete list of assays with IDs is given in Table S1).

Dex Injections in Mice

C57/BL mice (male, 10 weeks) were administered 10 mg/kg of dexamethasone (Sigma) via intraperitoneal injections. Hearts were extracted after 1 or 24 hours for protein and mRNA analysis.

Statistics

Statistical differences between groups were calculated using an unpaired, 2-tailed Student t test (Excel software). $P < 0.05$ was considered significant. Data analysis and statistics for ChIP-Seq and RNAseq are included in their respective sections.

Results

Dex-Induced Nuclear Translocation of GR Is Associated With Cardiomyocyte Hypertrophy

To determine the expression pattern and dynamics of GR in cardiomyocytes, we treated neonatal rat ventricular

cardiomyocytes with dexamethasone for 1, 6, and 24 hours. We observed nuclear translocation of GR by 1 and 6 hours, followed by diffuse cytosolic and nuclear distribution by 24 hours (Figure 1A). We also confirmed the dex-induced cytoplasmic-to-nuclear translocation of GR by Western blotting (Figure 1B and 1C). We observed a significant increase in cardiomyocyte surface area after 24 hours of dex treatment indicating cardiomyocyte hypertrophy (Figure 1D), which is consistent with the study by Ren et al¹⁰ showing similar changes in phenotype in H9c2 cells and neonatal cardiomyocytes with dex treatment for 72 hours. In addition, we confirmed similar translocations and increases in cell size in adult mouse ventricular cardiomyocytes in the presence of dex from increasing time periods of 1 and 24 hours (Figure S1A through S1C). These results suggest that dex is sufficient to induce nuclear GR translocation and cardiomyocyte hypertrophy.

GR ChIP-Seq Identifies 11 658 GR Binding Sites Associated With 6482 Genes After Dex Treatment

To identify transcriptional targets of GR, we performed ChIP-Seq with antibody against GR in isolated neonatal cardiomyocytes and treated them with ethanol (control) or dex (100 nmol/L) for 1 hour. The data revealed 11 658 merged active regions (overlapping intervals) of genomic GR binding sites (gGRBs) in ethanol-treated (control) and dex-treated cardiomyocytes. Of those, 11 628 regions were unique only to dex-treated cardiomyocytes, 2 to control cardiomyocytes, and 28 regions were common to both (Figure 2A). We compared the peak size metrics and correlation in these active regions by tabulating the number of tags that showed a significant increase after dex versus control (shown as box plot in Figure 2B). Similarly, we generated heat maps to determine tag distributions across active regions (Figure S2A). In addition, we graphed cumulative average values across the transcription start sites and gene bodies (Figure S2B) for control and dex-treated cardiomyocytes and input samples. These data showed significant enrichment of tags (gGRBs) in dex-treated samples versus control, especially near transcription start sites. The number of gGRBs we identified in cardiomyocytes was similar to those reported in mouse mammary cells and pituitary AtT-20 cells, showing 8236 binding sites after 1 hour of dex,³³ and in A549 human lung epithelial cells with 4392 and 29 432 sites after 1 and 3 hours of dex, respectively.^{34,35} Motif search using MEME/TOMTOM with the top 1000 peaks from GR ChIP-Seq data identified Glucocorticoid response element (GRE) with an E-value of 1.1×10^{-580} (Figure S2C).³⁶ Next, we correlated these GR binding sites with annotated genes. A GR binding region within the gene 10 kb upstream or 10 kb downstream of the gene

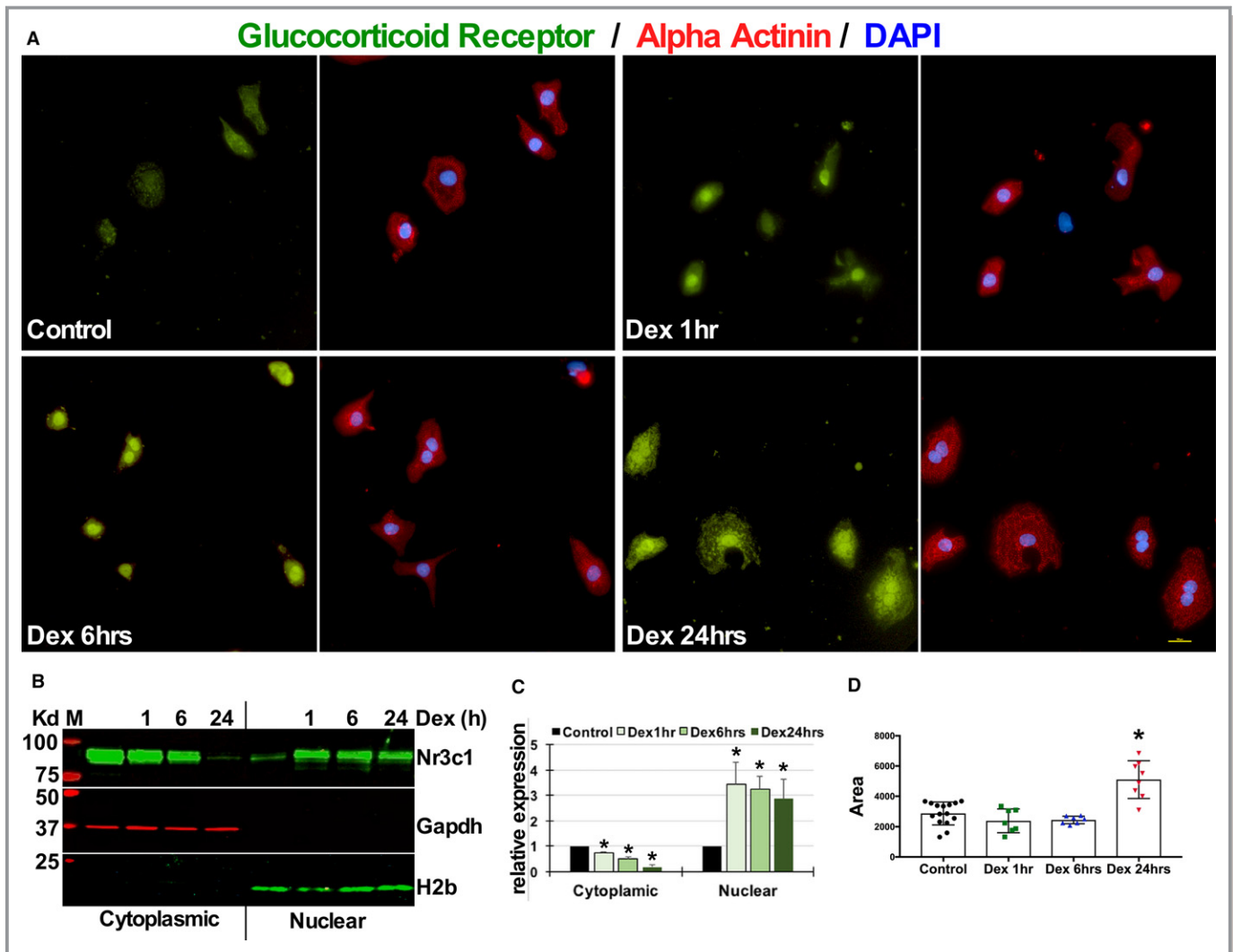


Figure 1. Dexamethasone induces nuclear translocation of the glucocorticoid receptor that is associated with cardiomyocyte hypertrophy. **A**, Neonatal rat ventricular cardiomyocytes were treated with dexamethasone (100 nmol/L) or ethanol for increasing time periods of 1, 6, or 24 hours before fixing and staining for glucocorticoid receptor, α -actinin (myocyte specificity), and DAPI (nucleus). Scale bar 10 μ mol/L. **B**, Western blot showing cytoplasmic and nuclear fractions of neonatal rat ventricular myocytes cultured and treated with dexamethasone for increasing time periods of 1, 6, and 24 hours. Blots probed for glucocorticoid receptor (Nr3c1, nuclear receptor subfamily 3 group C member 1), GAPDH, and histone 2b. **C**, Signal intensities of the cytoplasmic glucocorticoid receptor normalized to GAPDH and nuclear glucocorticoid receptor normalized to histone 2b are shown. ImageJ was used for quantification. **D**, Graph represents cardiomyocyte area as measured using ImageJ software, tabulated and graphed in Prism 7 (GraphPad, La Jolla, CA) to show change in cell size with dexamethasone treatments, as indicated. All experiments shown were repeated as independent triplicates, * $P < 0.05$. Dex indicates dexamethasone; GR, glucocorticoid receptor; H2b, histone 2b.

structure was considered associated with that gene and to possibly have regulatory influence on that gene's transcription. Interestingly, when we compared average peak value of dex versus control cardiomyocytes, 99.91% of genes (7075 out of 7080) showed ratios ≥ 1 (Figure 2C), suggesting an increase in GR tags after dex, and only 0.08% (6 out of 7080) had ratios < 1 , that is, dex decreased GR tags versus control (Figure 2D). Of the 7080 genes, 6482 genes showed a ≥ 2 -fold change in GR occupancy and were associated with at least 1 active region; interestingly, 6481 genes showed increase ($\text{Log}_2\text{FC} > 1$) in

gGRb, and only 1 gene showed a decrease ($\text{Log}_2\text{FC} < 1$) with dex treatment. Our data showed that a majority of these genes (66%) were associated with only 1 active region, while 34% had > 1 active region (Figure S2D). Next, we generated a pie chart that showed the distribution of peaks in control and dex-treated samples to determine the location of peaks with respect to genomic annotations (Figure S2E). These results for the first time reveal widespread gGRb on the cardiac genome after dex stimulation and conceivably identify genes that are regulated and contribute to dex-induced cardiac hypertrophy.

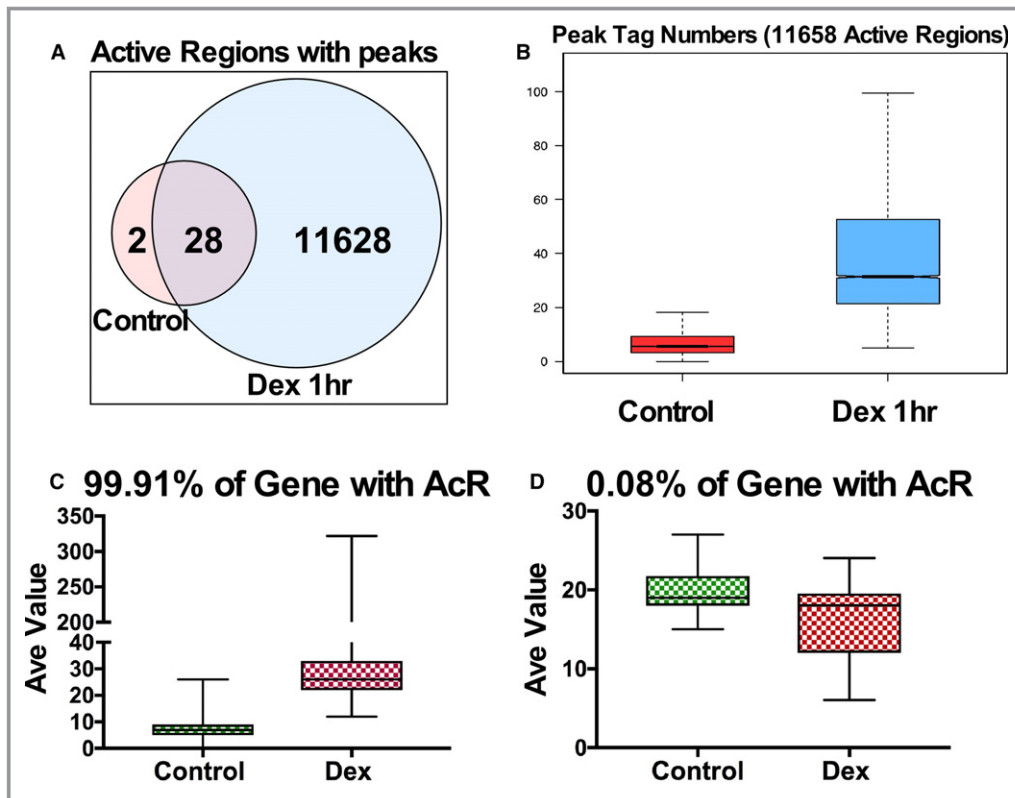


Figure 2. Genomic GR binding sites identified by GR ChIP-Seq in cardiomyocytes after 1 hour of Dex treatment. **A**, Venn diagram showing the number of active regions (actual binding sites) in control (ethanol) and dexamethasone (Dex, 100 nmol/L)-treated rat ventricular neonatal cardiomyocytes. **B**, Box plot comparing peak tag numbers in control and Dex-treated samples. Boxed area represents center 2 quartiles, notched line is median, and the whiskers show the top and bottom quartiles without outliers. **C**, Box plot showing average peak density in genes (99.91% of genes with active regions) sorted based on the ratio ≥ 1 in Dex-treated vs control samples. **D**, Box plots showing average peak density in genes (0.08% of genes with active regions) sorted based on ratio ≤ 1 in Dex-treated vs control samples. AcR indicates active regions; Ave, average; ChIP-Seq, chromatin immunoprecipitation sequencing; Dex, dexamethasone; GR, glucocorticoid receptor.

Early Targets of GR Include Regulators of RNA pol II-Dependent Transcription and Gene Expression in Cardiomyocytes

Our GR ChIP-Seq data identified 6482 genes associated with gGRb in cardiomyocytes after dex treatment. Therefore, to determine changes in transcriptional status, we performed RNAseq on isolated neonatal ventricular cardiomyocytes (2 independent cultures, $n=2$) treated with ethanol or dex for 1 or 24 hours. We selected these time points for transcriptome analysis because 1 hour is sufficient for maximum GR nuclear translocation, and we observed significant increase in cardiomyocyte size by 24 hours, indicating cardiomyocyte hypertrophy. Of the 11 546 transcripts that were sequenced, a total of 738 showed significant change (q -value < 0.5) with dex. After 1 hour, 98 genes ($< 1\%$ of all sequenced transcripts and 13.39% of those differentially regulated) exhibited a change in transcript abundance (Figure 3A and

Figure S3). After 24 hours, 640 additional genes (5.54% of all sequenced transcripts and 86.72% of those differentially regulated) showed a change in transcript abundance; there were also 55 genes that were common to both time points (Figure 3A). We generated a heat map using Log2FC values to show the differential change in gene expression after 1 and 24 hours of dex versus control in cardiomyocytes (Figure 3B, Table S2).

Further, we correlated expressed genes with their gGRb status, which showed that 358 (48.5%) differentially regulated genes were associated with gGRb, whereas 380 genes did not show gGRb in or within 10 kb upstream or downstream of their gene structure (Figure 4A). Interestingly, 5744 genes did associate with GR but did not show significant change (< 2 -fold change) in transcript abundance or were not identified in RNAseq (Figure 4A). These results are consistent with the study in A549 cells, which reported that 84% of the 10 963 GR binding sites tested showed less

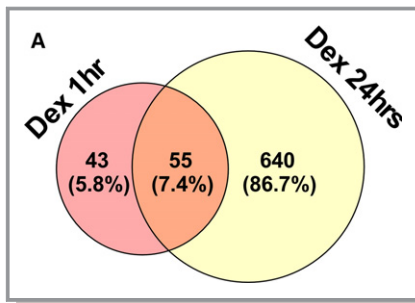


Figure 3. Differential transcriptome in cardiomyocytes treated with Dex for 1 and 24 hours. **A**, Venn diagram showing numbers and percentages of mRNA transcripts differentially regulated in cardiomyocytes treated with dexamethasone for 1 and 24 hours, along with transcripts changed under both conditions, compared with control cells, as measured by RNAseq. **B**, Heatmap displaying the 739 differentially regulated genes in cardiomyocytes treated with dexamethasone for 1 or 24 hours vs control (ethanol). Heatmap was generated using HeatMapper, with Complete linkage clustering method and Euclidean method for distance measurement. Dex indicates dexamethasone; Log2FC, log₂-fold change.

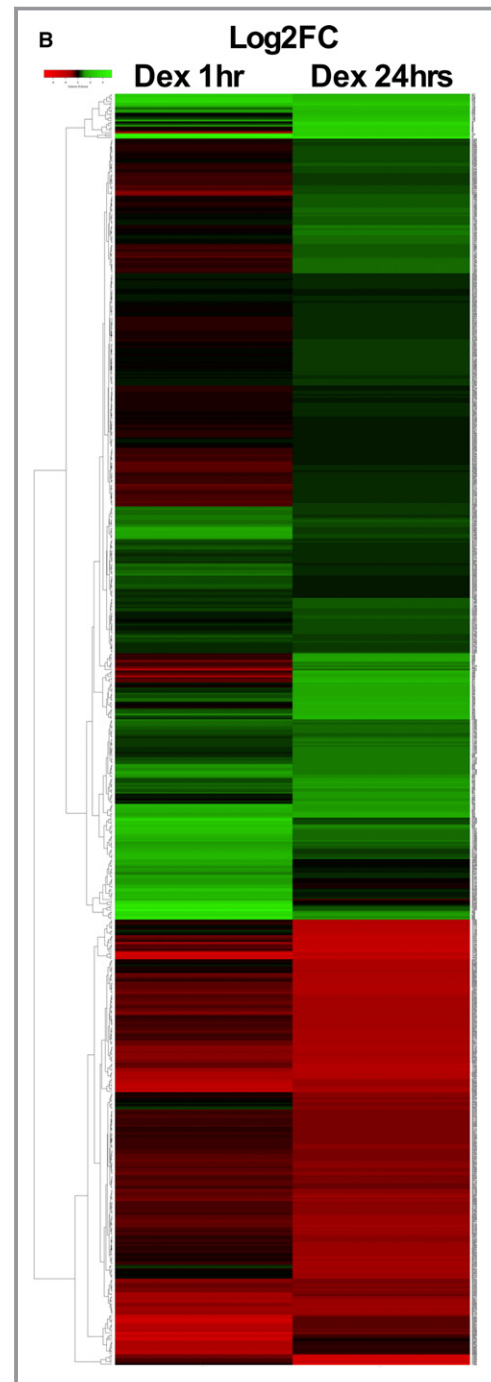


Figure 3. Continued

than a 2-fold change in reporter assay, suggesting “modest” change due to GR regulatory activity.³⁵ Further, we correlated 738 differentially regulated genes at the 2 measured time points with their gGRb status. After 1 hour of dex treatment, 68 of 98 (69.38%) genes with significant change were associated with gGRb, whereas 30 (30.61%) genes showed no association to gGRb. On the other hand, after 24 hours of dex, 290 out of 640 (45.31%) differentially regulated genes were associated with gGRb, whereas 350 (54.69%) genes were not associated with gGRb (Figure 4B). These data suggest that activation of GR signaling in cardiomyocytes results in an initial change in expression of mostly direct targets of GR followed by more genes that are either indirect targets or secondary to hypertrophy phenotype. In Figure 4C, we show the graph with Log₂FC values of 68 genes that exhibit significant differential regulation (Log₂FC ≥ 1) and gGRb at 1 hour and the corresponding changes after 24 hours of dex compared with control cardiomyocytes (Figure 4C and Figure S3). In Figure 4D, we show representative screenshot images of *Pdk4*, *Abra*, *Sgk1*, *Klf10*, and *Hes1* genes from an integrated genome viewer that are differentially regulated by 1 hour of dex and are associated with gGRb (Figure 4D). We confirmed the change in mRNA abundance of selected genes listed in this group in cardiomyocytes treated with dex for increasing time periods of 1, 6, and 24 hours (Figure 4E). Interestingly, gene ontology for functional annotation using

DAVID (Database for Annotation, Visualization and Integrated Discovery) Bioinformatics Resources 6.8^{37,38} categorized these genes as regulators of gene transcription from RNA polymerase II promoter, followed by those involved in cell death, response to lipopolysaccharide, and mechanical or insulin stimulus (Figure 4F, Figure S4). Previous studies have shown association of these genes, such as *Abra*,³⁹ *Klf10*,⁴⁰ *Pdk4*,⁴¹ and *Sgk1*⁴² in development of hypertrophic cardiomyopathy.

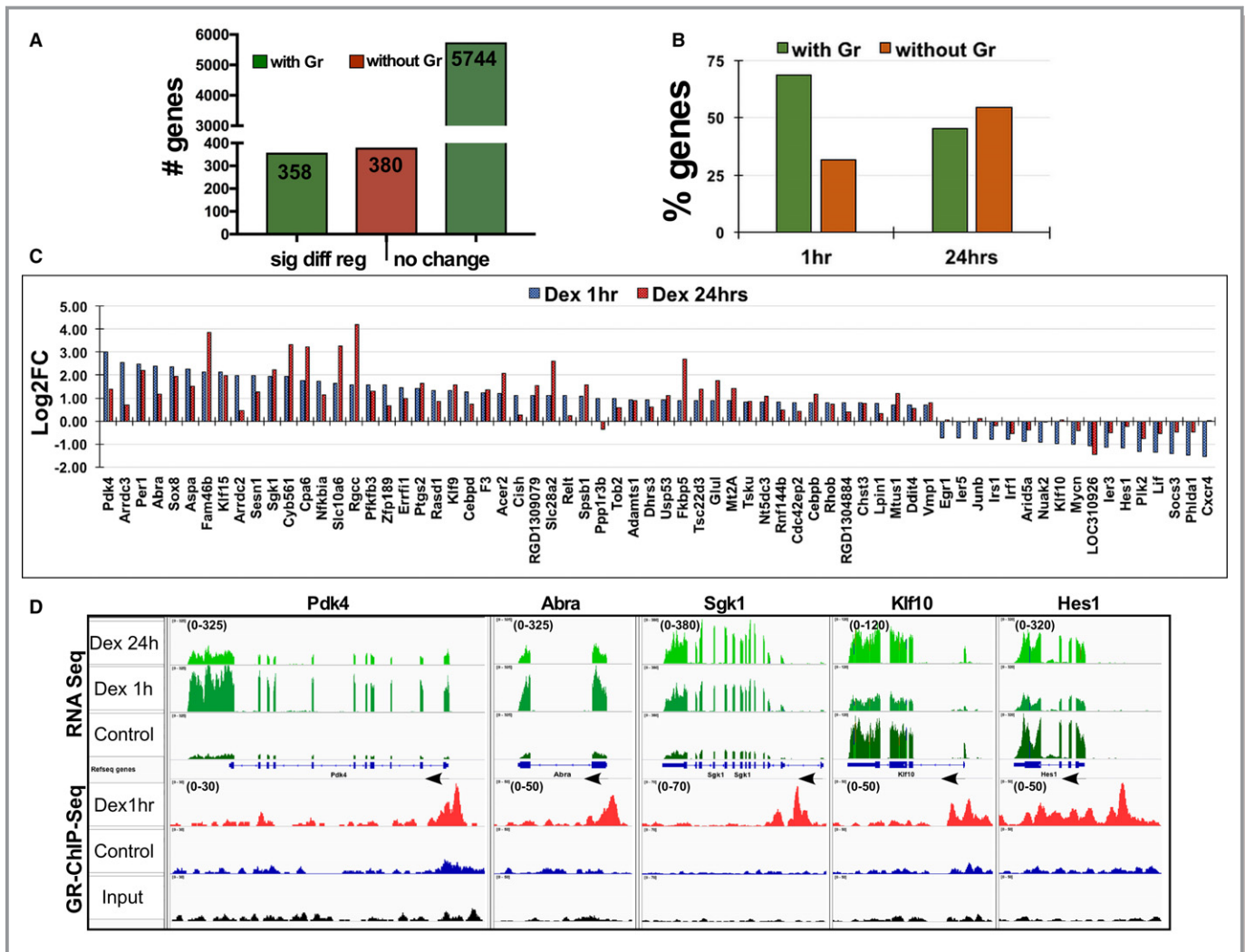


Figure 4. Early targets of GR include regulators of pol II-dependent transcription and gene expression in cardiomyocytes. **A**, The graph represents the numbers of genes with or without GR association, sorted into genes that show significant differential regulation and genes that do not show significant change in transcript abundance. **B**, The graph represents the number of genes differentially regulated and the status of GR genomic association at the 1-hour and 24-hour time points of dexamethasone treatment. **C**, Genes with significant change in mRNA transcript that are associated with genomic GR binding at 1 hour along with corresponding change after 24 hours of dexamethasone treatment are graphed and presented based on log₂-fold change (Log₂FC) value. **D**, Integrated genomic viewer screenshots of selected representative genes with integrated RNAseq and GR ChIP-Seq data, showing change in the transcript after 1 and 24 hours of dexamethasone along with genomic GR binding status of genes that are differentially regulated at 1 hour dexamethasone treatment compared with control (ethanol) cardiomyocytes. Arrows indicate the direction of transcription of that gene, numbers in brackets in the Y axis indicate the values on signal tracks for GR ChIP-Seq and RNAseq for each gene. The values were kept the same within the samples for each gene. **E**, Relative transcript abundance of selected genes as measured by quantitative polymerase chain reaction in cardiomyocytes treated with dexamethasone for 1, 6, or 24 hours. Error bars represent SEM, **P*<0.05 compared with control, n=3. **F**, Functional annotation of genes that show significant differential regulation after 1 hour of dexamethasone treatment that are associated with genomic GR, as analyzed using DAVID; top 15 groups are shown with number of genes and *P* value (full table with all the categorized genes in Figure S4). DAVID indicates Database for Annotation, Visualization and Integrated Discovery; Dex, dexamethasone; GR, glucocorticoid receptor.

Similarly, we graphed 30 genes that exhibit change in transcript abundance after 1 hour of dex but are not associated with gGRb, along with corresponding changes at 24 hours (Figure S5A). In Figure S5B, we show screenshot images from an integrated genome viewer browser showing representative genes from this group (Figure S5B). We confirmed the expression changes of these genes in neonatal

cardiomyocytes treated with dex for increasing time periods (Figure S5C). Interestingly, functional annotation revealed that most of these genes are involved in heart development, cell-cell junction organization, Ca²⁺ transport, and G protein-coupled receptor signaling (Figure S5D), some of which might be regulated via nongenomic actions of Gc-GR signaling. These data suggest that an early change in a small set of

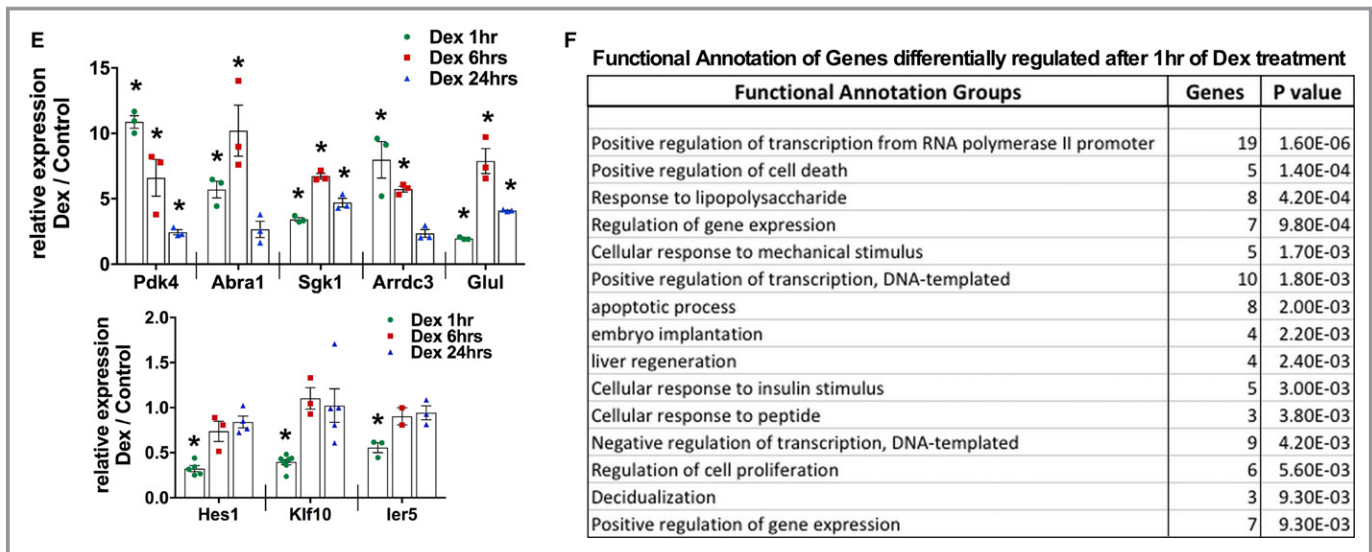


Figure 4. Continued.

genes with dex, mostly transcription regulators, might mediate change in expression of additional signaling genes, which potentially contribute to the development of cardiomyocyte hypertrophy.

Genes Mostly Involved in Growth-Related Pathways and Cardiomyopathy Differentially Regulated After 24 Hours of Dex Treatment

We examined genes that exhibit significant changes only after 24 hours of dex, which includes genes with and without gGRb association (Figure 4B). We plotted graphs of these genes with Log2FC values to show the corresponding changes in the transcript after 1 and 24 hours of dex (Figure 5A; Table S3). As anticipated by the hypertrophy phenotype, functional annotation (DAVID) grouped these genes as mostly those that are involved in focal adhesion, extracellular matrix–receptor interaction, dilated and hypertrophic cardiomyopathy, and other growth-related pathways such as PI3K–Akt signaling, adrenergic signaling in cardiomyocytes, insulin signaling, calcium signaling pathways, and Hippo signaling (Figure 5B, Figure S6). We validated the expression of selected relevant genes from the RNAseq by qPCR in cardiomyocytes treated with dex for increasing time periods of 1, 6, and 24 hours (Figure 5C). We show screenshots of relevant representative genes as visualized on an integrated genome viewer browser displaying integrated RNAseq and GR–ChIP–Seq data. In Figure 5D, *Myoz2* and *Myocd* are shown as examples of differentially regulated genes and associated with gGRb, and Figure 5E shows *Agtr1a*, *Ace*, and *MyI2* as genes changed by not associating with gGRb. These genes could be direct or indirect targets of GR; alternatively, these changes could be secondary to the hypertrophy phenotype we observed after

24 hours of dex treatment. Nevertheless, these results indicate that Gc stimulation in cardiomyocytes leads to change in the transcriptome that is involved in the development of cardiomyocyte hypertrophy.

Majority of Genes With Genomic GR Binding Show Incremental Changes in Transcript Abundance and Are Categorized as Genes Involved in Basic Cellular Processes

Our ChIP–Seq data revealed at least 6482 genes that are associated with gGRb, which resulted in significant differential regulation in 738 genes (11.38%); 5744 genes (88.61%, including genes with no significant difference in mRNA abundance and transcripts that did not sequence) did not show significant change. Of the latter set of genes, 4954 (76.42%) passed the quality check and were included in further analysis. Functional annotation identified these genes as mostly involved in basic cellular processes such as protein processing in endoplasmic reticulum, spliceosome, the MAPK signaling pathway, proteasomes, ubiquitin-mediated proteolysis, ribosomes, and metabolic pathways (Figure 6A and Figure S7). In Figure 6B, we show *Trapp6b*, *Pnn*, *Scd4*, *Rab12*, *Sumo2*, and *Mapk1* as representative genes with associated gGRb but no significant change in transcript abundance (Figure 6B). We confirmed the expression of these genes, which showed a slight change of 1.15- to 1.3-fold in mRNA levels (Figure 6C), consistent with a report in A549 cells showing modest changes in regulatory activity for most GR binding sites.³⁵ Interestingly, these genes overlapped with genes that are regulated by promoter clearance of paused RNA pol II in hearts undergoing hypertrophy (Figure S8A)²⁶ and possibly might be undergoing similar transcriptional

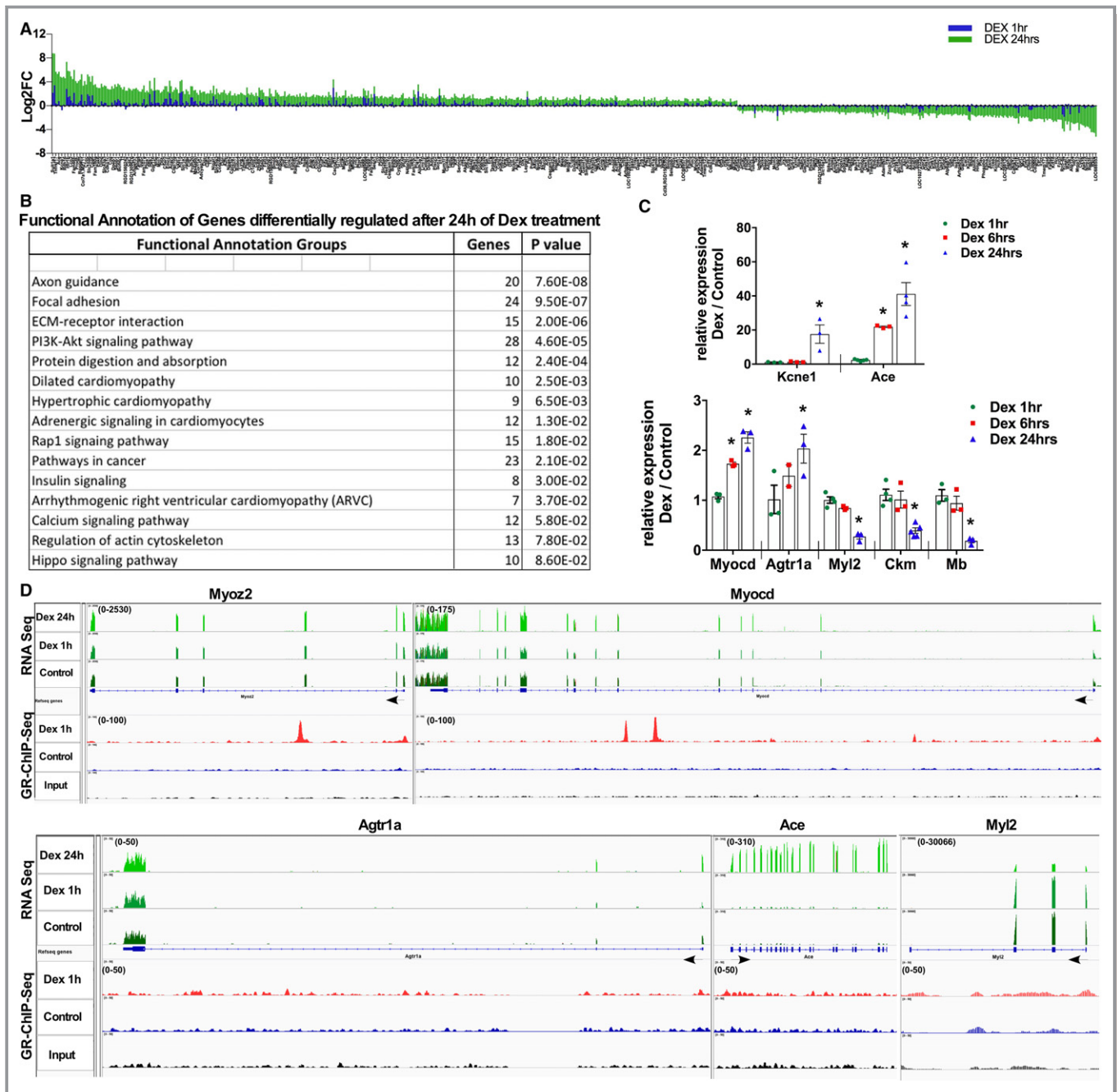


Figure 5. Genes involved in growth-related pathways and cardiomyopathy are differentially regulated after 24 hours of dexamethasone treatment. **A**, Graph represents genes that are differentially regulated at 24 hours, along with the corresponding changes at 1 hour of dexamethasone treatment in cardiomyocytes (gene list provided as Table S3). **B**, Functional annotation of genes regulated only after 24 hours of dexamethasone treatment were analyzed using DAVID, and relevant groups with number of genes and *P* value are shown (all categorized groups shown in Figure S6). **C**, Transcript abundance of selected genes as measured by qPCR in neonatal ventricular cardiomyocytes treated with dexamethasone for 1, 6, or 24 hours. Error bars represent SEM, **P*<0.05 compared with control, n=3. **D**, Integrated genomics viewer screenshots of selected representative genes with RNAseq and GR ChIP-Seq data, showing change in the transcript after 1 and 24 hours of dexamethasone along with genomic GR binding status of these genes at 1 hour of dexamethasone treatment compared with control (ethanol) cardiomyocytes. ChIP-Seq indicates chromatin immunoprecipitation sequencing; DAVID, Database for Annotation, Visualization and Integrated Discovery; Dex, dexamethasone; GR, glucocorticoid receptor; qPCR, quantitative polymerase chain reaction; RNAseq, RNA sequencing.

regulation in cardiomyocytes with dex treatment. On the other hand, genes with significant differential change and gGRb association after 1 hour of dex in cardiomyocytes (eg, *Abra*,

Pdk4, *Klf10*, *Hes1*) displayed overall change in RNA pol II recruitment and distribution on gene structures in vivo with hypertrophy compared with sham hearts (Figure S8B).²⁶ RNA

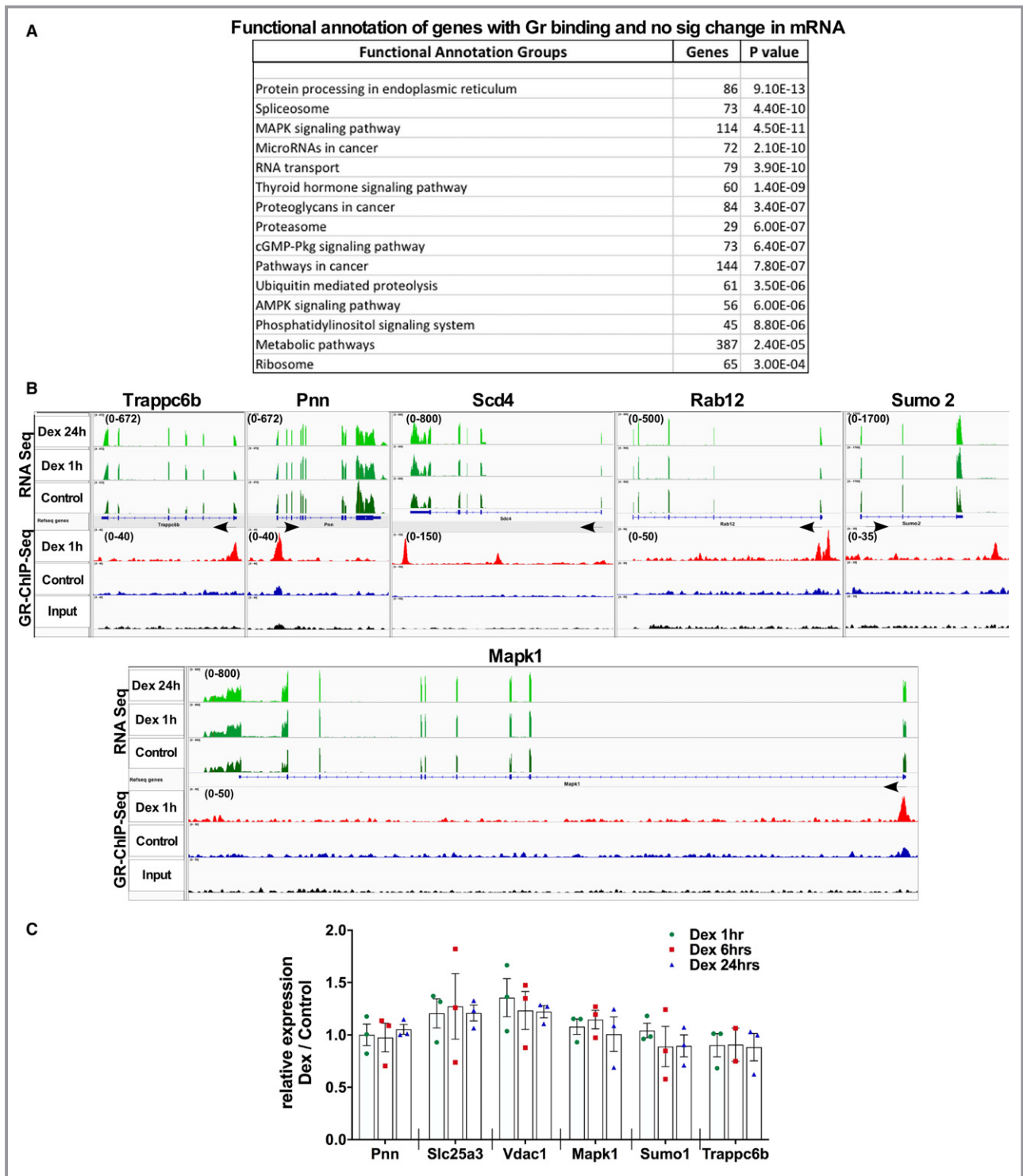


Figure 6. Incremental changes in most of genes with genomic GR association in cardiomyocytes with dexamethasone treatment. **A**, Functional annotation of genes that show less than a 2-fold change in transcript abundance and are associated with genomic GR binding; groups with number of genes and *P* value are shown (all categorized groups shown in supporting information). **B**, Integrated genomics viewer screenshots of selected representative genes with RNaseq and GR ChIP-Seq data, showing change in the transcript after 1 and 24 hours of dexamethasone along with genomic GR-binding status of these genes at 1 hour of dexamethasone treatment compared with control (ethanol) cardiomyocytes. **C**, Transcript abundance of selected genes as measured by qPCR in neonatal ventricular cardiomyocytes treated with dexamethasone for 1, 6, or 24 hours. Error bars represent SEM, *n*=3. ChIP-Seq indicates chromatin immunoprecipitation sequencing; Dex, dexamethasone; GR, glucocorticoid receptor; qPCR, quantitative polymerase chain reaction; RNaseq, RNA sequencing; sig, significant.

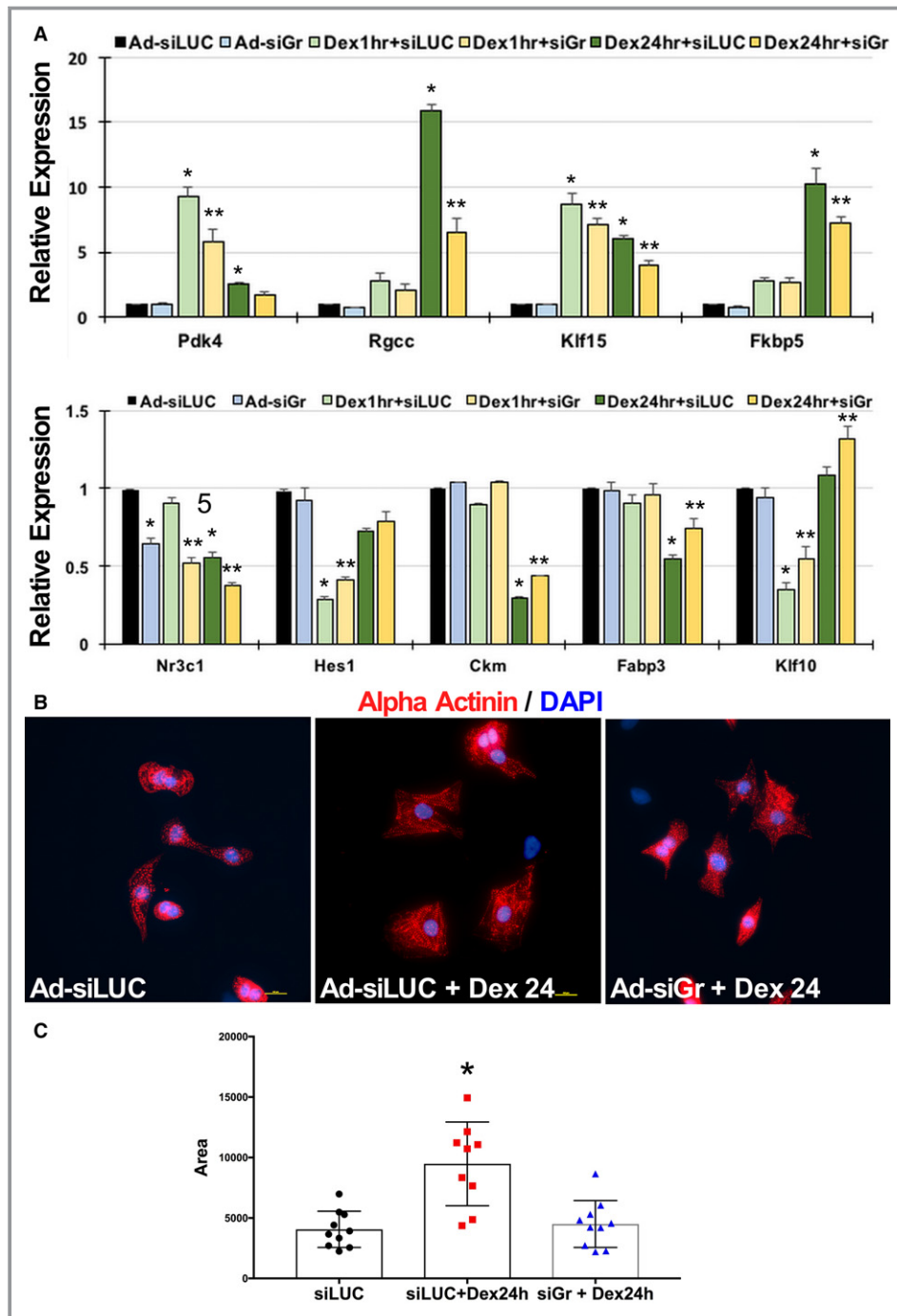


Figure 7. Dexamethasone-mediated change in cardiomyocyte gene transcription and morphology are GR-dependent. **A**, Isolated neonatal rat ventricular cardiomyocytes were infected with adenovirus expressing short hairpin RNA against GR (Ad-siGr) for 24 hours before treatment with dexamethasone for 1 or 24 hours, as indicated. Transcript abundance was measured by qPCR of selected representative genes that show differential regulation at 1 or 24 hours, with or without association with genomic GR binding. Error bars represent SEM, and * is $p < 0.05$ vs. control and ** is $p < 0.05$ vs. respective dex treatment. **B**, Isolated neonatal rat ventricular cardiomyocytes plated on glass slides were treated with Ad-siGr for 24 hours before dexamethasone treatment for 24 hours. Slides were fixed and stained for α -actinin or DAPI. Scale bar 10 μ m. **C**, Graph represents cardiomyocyte area as measured using ImageJ software, tabulated and graphed to show change in cell size with treatments, as indicated. Ad-siLUC indicates adenovirus expressing short hairpin RNA against luciferase (LUC); Dex, dexamethasone; GR, glucocorticoid receptor; qPCR, quantitative polymerase chain reaction.

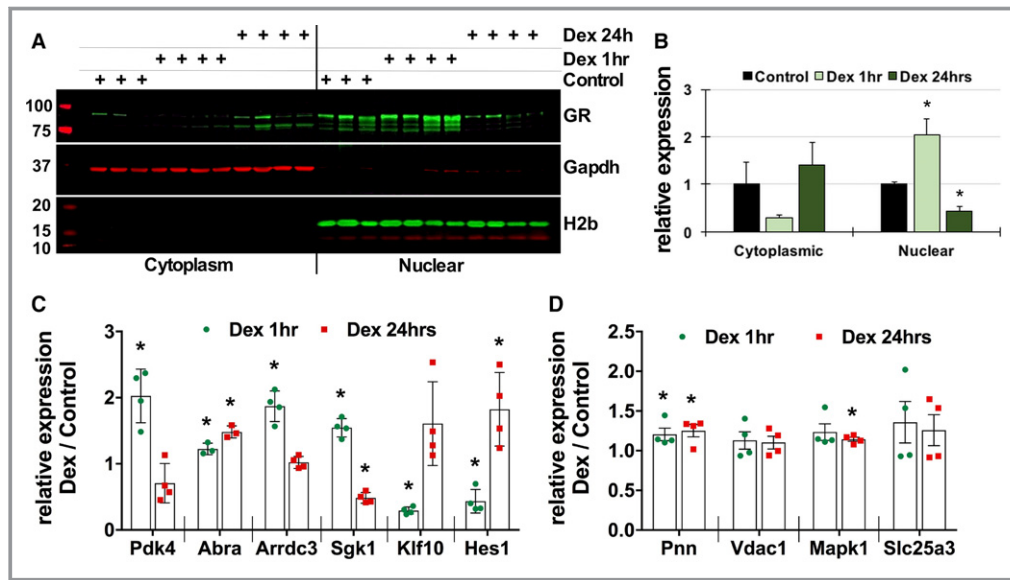


Figure 8. Dexamethasone injections result in similar transcriptional changes in mouse hearts as seen in isolated cardiomyocytes. **A**, Western blotting showing GR expression and translocation in mouse hearts after intraperitoneal injections of dexamethasone (10 mg/kg) for 1 or 24 hours. GAPDH and histone 2b were used for compartment specificity and as loading controls. Control n=3, dexamethasone injections n=4, each time point. **B**, Graph represents GR signal intensity normalized to the respective loading controls and presented as relative to the compartmental control samples. Control n=3 and Dex injections n=4, each time point. **C** and **D**, Transcript abundance of selected genes as measured by qPCR in hearts treated with dexamethasone for 1 or 24 hours. Error bars represent SEM, * $P < 0.05$ compared with control, n=3 (control), 4 (dexamethasone, each time point). Dex indicates dexamethasone; GR, glucocorticoid receptor; H2b, histone 2b; qPCR, quantitative polymerase chain reaction.

pol II-ChIP-qPCR on representative genes (*Trapp6b* and *Mapk1*) showed a decrease in RNA pol II occupancy at the transcription start site of these genes with dex treatment (Figure S8C) accompanied by incremental changes in transcript, as shown in Figure 6C. Thus, we propose that the expression of these genes might be regulated by promoter clearance of paused pol II.

Further, to confirm that the dex-induced changes in the transcriptome and hypertrophic phenotype were mediated by GR, we silenced endogenous GR using adenovirus expressing shRNA against GR before treating cardiomyocytes with dex for 1 or 24 hours. As expected, we observed a blunted dex response with respect to expression of the target genes (Figure 7A) and cardiomyocyte hypertrophy (Figure 7B and C). These results indicate that the GR-dependent change in transcriptome contributes to development of dex-induced cardiomyocyte hypertrophy.

Ingenuity Pathway Analysis of Dex-Regulated Genes in Cardiomyocytes

We analyzed the RNAseq data using Ingenuity Pathway Analysis software (IPA, Qiagen, Hilden, Germany) for associated signaling pathways and networks. As seen with DAVID analysis, the 1-hour time point showed mostly genes that

were involved in transcriptional regulation. Figure S9A shows a network of genes that regulate transcription, along with their subcellular localization, and change with dex versus control (green is decreased, red increased). Interestingly, almost all genes that have been predicted to inhibit transcription (shown with blue dotted lines) are decreased with dex (Figure S9A), suggesting overall transactivation of transcriptome. We did a similar analysis of the genes that showed differential regulation after 24 hours of dex compared with control cardiomyocytes. IPA listed these genes as involved in cardiac hypertrophy, cardiac failure, cardiac necrosis/cell death, and toward the top of the toxicity list (Figure S9B). IPA toxicity analysis links data to clinical pathology end points using custom toxicity lists and functional groups, thus predicting the association of genes with the relevant clinical pathologies. The figure also shows the top 20 from the list as a bar graph, where a higher $-\log(P\text{-value})$ indicates higher significant association, with threshold $P=0.05$ (Figure S9B). We generated a network using the genes categorized under cardiac hypertrophy, which showed “enlargement of heart” as the first group with 54 genes, followed by heart failure, cardiac dysfunction, and infarction (Figure S9C and S9D, top table). Cardiovascular disease was also listed second in the list for the top diseases and disorders that were associated with the genes that showed change after

24 hours with dex (Figure S9D, middle table). IPA analysis listed cardiovascular system development and function on top of the list with 201 genes, followed by organismal development and survival, and skeletal and muscular system development for physiological system development and function (Figure S9D, lower table).

In Vivo Dex Injection Results in Similar Transcriptional Changes in Mouse Hearts as Seen in Isolated Cardiomyocytes

To examine the effects of dex-induced GR-mediated transcriptional changes in vivo, we administered mice with dex (10 mg/kg) via intraperitoneal injections. There was no obvious increase in heart weight/body weight or tibia length after 1 or 24 hours of dex injections (Figure S8D), and no significant increase was observed in *Myh7*; there was a slight but significant decrease in *Myh6* only after 24 hours (Figure S8E). We confirmed increase in nuclear GR with dex by Western blotting (Figure 8A and 8B). Not surprisingly, we observed similar transcriptional changes in hearts treated with dex as seen in isolated cardiomyocytes. Significant increases were seen in genes that showed differential regulation in cardiomyocytes after Dex treatment (Figure 8C), and genes involved in basic cellular processes showed modest changes in transcript levels, mimicking our in vitro results from cardiomyocytes treated with dex (Figure 8D).

Based on our results, we conclude that dex treatment in cardiomyocytes initially (1 hour) causes a change in the expression of genes that are mostly direct GR targets (68 out of 98), of which at least 37% are known transcriptional regulators. After 24 hours, 54% of differentially regulated genes are not associated with GR genomic binding and could be indirect GR targets or secondary to developing hypertrophy. These changes in transcriptome induce and contribute to the GR-dependent cardiomyocyte hypertrophy.

Discussion

Gcs, “stress hormones” secreted from the adrenal cortex, affect almost all tissues by acting as a ligand to nuclear receptor subfamily 3, group C, member 1 to mediate transcriptional changes of target genes. High levels of circulating corticosteroids due to an increase in endogenous secretion or exogenous administration for long periods can lead to the condition known as Cushing syndrome or hypercortisolism, which is characterized by hypertension, obesity, diabetes mellitus, weak and atrophic muscles, along with other physical manifestations.⁴³ Case studies have shown congestive cardiac failure with left ventricular hypertrophy and dysfunction in these individuals, with reversal of the observed phenotype following correction of hypercortisolism.⁴⁴⁻⁴⁷

Synthetic corticosteroids are frequently used in clinics as potent anti-inflammatory agents, with treatment schedules extending from single doses to extended periods of time. Although the contribution of Gcs in development and disease has been studied before, the advent of new, advanced genome-wide sequencing technologies has allowed a more detailed examination of the downstream targets, transcriptional changes, and the phenotypic outcome of Gc-GR signaling. In this study we examined GR signaling in cardiomyocytes using high-throughput GR ChIP and RNA sequencing on the cardiac genome and resulting changes in the transcriptome. Here we report the full array of target genes that are regulated with dex treatment along with GR genomic binding dynamics.

Our GR ChIP-Seq data identified 11 658 active regions/binding sites correlating with 7080 genes, of which 6482 genes show >2-fold change in GR peak value in the cardiac genome after dex treatment for 1 hour compared with control. These data are in agreement with reports in mouse mammary cells and pituitary AtT-20 cells showing 8236 binding sites after 1 hour of dex³³ and A549 human lung epithelial cells with 4392 and 29 432 sites after 1 and 3 hours of dex, respectively.^{34,35} We speculate that the difference in number of sites identified could be due to differences in chromatin accessibility in terminally differentiated cardiomyocytes versus proliferating cell lines, or it may be due to technical differences in ChIP reaction or depth of sequencing. A recent study examined co-occupancy of cardiac transcription factors in HL1 cells, which showed number of peaks ranging from 56 362 for TBX5 to 1339 for Mef2A.⁴⁸ Therefore, even with large coverage and binding regions in the cardiac genome, Glucocorticoid Response Element (GRE) is not the top predicted transcription factor binding site.

Our RNAseq data also agree with the study in A549 cells, where Reddy et al saw differential regulation of 209 genes after 1 hour of dex and identified mostly genes involved in transcription regulation from the pol II promoter, apoptosis, anatomical structural development, and regulation of gene expression.³⁴ Our RNAseq data with the 24-hour time point identified novel genes involved in growth-related signaling pathways, such as calcium signaling or regulation of actin cytoskeletal regulation, that contribute to the hypertrophic phenotype along with other known hypertrophic pathways. In 2012 Ren et al examined genes regulated by dex treatment after 6, 24, and 48 hours in H9c2 cells cultured under serum and serum-free conditions by microarray analysis.¹⁰ In contrast to our results, which showed changes in transcript levels of 695 genes, microarray data in the Ren et al study showed differential regulation of 4793 genes and 2454 genes after the 24-hour time point in serum or serum-free conditions, respectively, of which 48 genes were associated with cardiac hypertrophy signaling by Ingenuity pathway

analysis.¹⁰ We confirmed the increase in 18% of these 48 genes in our neonatal rat cardiomyocytes treated with 24 hours of dex by RNAseq. We believe that the cell type, nature of culturing conditions and treatments, and the method of transcriptome analysis could explain the difference in the data output, however, we did observe the same phenotype of increase in cell size after 24 hours of dex treatment. Cardiac-specific GR knockout mice develop left ventricular dilatation, atrial thrombosis and fibrosis, and systolic dysfunction as early as 3 months of age with development of fulminant cardiac failure by 6 months, indicating that Gc-GR signaling is essential for the prevention of heart disease.¹⁴ This agrees with the critical role of glucocorticoid signaling at birth, where Gc mediates the switch of heart growth from cardiomyocyte proliferation to hypertrophy.⁷

This is the first study correlating GR ChIP-Seq and RNAseq data in cardiomyocytes, through which we have identified novel genomic targets of GR in cardiomyocytes after 1 and 24 hours of dex. An interesting observation was that a majority of genes (88.61%) with GR association did not show a significant change in transcript abundance. These data agree with results by Vockley et al, who used a reporter assay to show that 84% of the gGRb results in a modest change in reporter activity.³⁵ Gene ontology categorized these genes as those that are involved in basic cellular processes and expressed constitutively in cardiac cells under physiological and hypertrophic conditions, which is noteworthy because our previous study in mice showed similar changes in these genes mediated by promoter clearance of paused RNA pol II in hypertrophied hearts compared with sham.²⁶ Although we did confirm a decrease in promoter RNA pol II occupancy with dex treatments in representative genes, which suggests clearance of paused RNA pol II, further examination of genome-wide pol II occupancy and epigenetic changes is needed to verify the proposed mechanisms of regulation of these genes with gGRb but modest changes in transcription. Promoter proximal RNA pol II pausing has been shown to be widespread as a rate-limiting step for transcription.^{26,49,50} Thus, GR association to these genes might be regulating this transcriptional mode, resulting in small changes in transcriptional output that may be required, and might contribute to cardiomyocyte hypertrophy.

We identified several novel direct and secondary targets of GR in cardiomyocytes, such as *Abra1*, *Klf10*, and *Lrrc10*, along with several others that have not previously been associated with Gc-GR signaling, to the best of our knowledge. *Abra1* (the gene encoding actin-binding rho-activating protein), also known as Myocyte Stress-1 (MS1) or striated muscle activator of Rho signaling, was identified as a gene that is highly expressed in muscle within 4 hours of pressure overload, before an actual increase in heart weight, which suggests a role in the induction of cardiac hypertrophy.³⁹ Subsequent studies further confirmed the role of *Abra1* in the

development of cardiac and skeletal muscle hypertrophy when these are subjected to work overload, where the gene mediates nuclear translocation of serum response factor coactivators, myocardin-related transcription factors A and B.^{51,52} Our data show that *Abra1* increases significantly after 1 and 24 hours of dex compared with control cardiomyocytes. Kruppel-like factor 10 (*Klf10*), also known as TGF β -inducible early gene-1, is a member of zinc finger family Kruppel-like transcription factors. *Klf10* functions as a tumor suppressor and antiproliferative in cancer cells.⁴⁰ *Klf10*-knockout male mice develop cardiac hypertrophy and fibrosis by 16 months of age.⁵³ *Klf10* mutations have also been associated with the development of hypertrophic cardiomyopathy in humans, which mimics the phenotype observed in knockout mice with respect to late onset.⁵⁴ We see an early decrease in *Klf10* after 1 hour of dex, which returns to normal levels by 6 hours and is maintained at 24 hours, suggesting a role in induction of cardiomyocyte growth. Studies have also shown involvement of other genes that are regulated as early as 1 hour, such as *Pdk4*⁴¹ and *Sgk1*,⁴² in the development of hypertrophic cardiomyopathy. With respect to the 24-hour time point, functional annotation of our data revealed change in growth-related pathways involving a network of several genes that are involved in the development of hypertrophy and failure.

In conclusion, in this study we have systematically characterized GR signaling and the resulting change in the transcriptome in cardiomyocytes. Moreover, we have identified known and novel targets of activated GR in cardiomyocytes, which play a role in the development of dex-induced cardiomyocyte hypertrophy.

Acknowledgments

We thank Dr Abdellatif, Professor, department of Cell Biology and molecular Medicine and Dr Sadoshima, Chair of the Department of Cell Biology and Molecular Medicine, Rutgers New Jersey Medical School, for support.

Author Contributions

E.S., S.A., and W.D. performed experiments; P.D. helped in IPA (Qiagen, Hilden, Germany) analysis of RNAseq data; N.S. was involved in article preparation; D.S. designed and performed experiments, performed data analysis with figures, and wrote the article.

Sources of Funding

This work was supported by National Institutes of Health funding to the corresponding author (1R01HL128799).

Disclosures

None.

References

- Munck A, Guyre PM, Holbrook NJ. Physiological functions of glucocorticoids in stress and their relation to pharmacological actions. *Endocr Rev*. 1984;5:25–44.
- Ong GS, Young MJ. Mineralocorticoid regulation of cell function: the role of rapid signalling and gene transcription pathways. *J Mol Endocrinol*. 2017;58:R33–R57.
- Funder JW. Glucocorticoid and mineralocorticoid receptors: biology and clinical relevance. *Annu Rev Med*. 1997;48:231–240.
- Pratt WB, Morishima Y, Murphy M, Harrell M. Chaperoning of glucocorticoid receptors. *Handb Exp Pharmacol*. 2006;172:111–138.
- Pratt WB, Toft DO. Steroid receptor interactions with heat shock protein and immunophilin chaperones. *Endocr Rev*. 1997;18:306–360.
- Echeverria PC, Picard D. Molecular chaperones, essential partners of steroid hormone receptors for activity and mobility. *Biochim Biophys Acta*. 2010;1803:641–649.
- Richardson RV, Batchen EJ, Denvir MA, Gray GA, Chapman KE. Cardiac GR and MR: from development to pathology. *Trends Endocrinol Metab*. 2016;27:35–43.
- Ohtani T, Mano T, Hikoso S, Sakata Y, Nishio M, Takeda Y, Otsu K, Miwa T, Masuyama T, Hori M, Yamamoto K. Cardiac steroidogenesis and glucocorticoid in the development of cardiac hypertrophy during the progression to heart failure. *J Hypertens*. 2009;27:1074–1083.
- Guder G, Bauersachs J, Frantz S, Weismann D, Allolio B, Ertl G, Angermann CE, Stork S. Complementary and incremental mortality risk prediction by cortisol and aldosterone in chronic heart failure. *Circulation*. 2007;115:1754–1761.
- Ren R, Oakley RH, Cruz-Topete D, Cidlowski JA. Dual role for glucocorticoids in cardiomyocyte hypertrophy and apoptosis. *Endocrinology*. 2012;153:5346–5360.
- La Mear NS, MacGilvray SS, Myers TF. Dexamethasone-induced myocardial hypertrophy in neonatal rats. *Biol Neonate*. 1997;72:175–180.
- Whitehurst RM Jr, Zhang M, Bhattacharjee A, Li M. Dexamethasone-induced hypertrophy in rat neonatal cardiac myocytes involves an elevated L-type Ca (2+) current. *J Mol Cell Cardiol*. 1999;31:1551–1558.
- Lister K, Autelitano DJ, Jenkins A, Hannan RD, Sheppard KE. Cross talk between corticosteroids and alpha-adrenergic signalling augments cardiomyocyte hypertrophy: a possible role for SGK1. *Cardiovasc Res*. 2006;70:555–565.
- Oakley RH, Ren R, Cruz-Topete D, Bird GS, Myers PH, Boyle MC, Schneider MD, Willis MS, Cidlowski JA. Essential role of stress hormone signaling in cardiomyocytes for the prevention of heart disease. *Proc Natl Acad Sci USA*. 2013;110:17035–17040.
- de Vries WB, van der Leij FR, Bakker JM, Kamphuis PJ, van Oosterhout MF, Schipper ME, Smid GB, Bartelds B, van Bel F. Alterations in adult rat heart after neonatal dexamethasone therapy. *Pediatr Res*. 2002;52:900–906.
- de Vries WB, Bal MP, Homoet-van der Kraak P, Kamphuis PJ, van der Leij FR, Baan J, Steendijk P, de Weger RA, van Bel F, van Oosterhout MF. Suppression of physiological cardiomyocyte proliferation in the rat pup after neonatal glucocorticosteroid treatment. *Basic Res Cardiol*. 2006;101:36–42.
- Rog-Zielinska EA, Thomson A, Kenyon CJ, Brownstein DG, Moran CM, Szumska D, Michailidou Z, Richardson J, Owen E, Watt A, Morrison H, Forrester LM, Bhattacharya S, Holmes MC, Chapman KE. Glucocorticoid receptor is required for foetal heart maturation. *Hum Mol Genet*. 2013;22:3269–3282.
- Gay MS, Dasgupta C, Li Y, Kanna A, Zhang L. Dexamethasone induces cardiomyocyte terminal differentiation via epigenetic repression of cyclin D2 gene. *J Pharmacol Exp Ther*. 2016;358:190–198.
- Macfarlane DP, Forbes S, Walker BR. Glucocorticoids and fatty acid metabolism in humans: fuelling fat redistribution in the metabolic syndrome. *J Endocrinol*. 2008;197:189–204.
- Yoshikawa N, Nagasaki M, Sano M, Tokudome S, Ueno K, Shimizu N, Imoto S, Miyano S, Suematsu M, Fukuda K, Morimoto C, Tanaka H. Ligand-based gene expression profiling reveals novel roles of glucocorticoid receptor in cardiac metabolism. *Am J Physiol Endocrinol Metab*. 2009;296:E1363–E1373.
- Takeshita Y, Watanabe S, Hattori T, Nagasawa K, Matsuura N, Takahashi K, Murohara T, Nagata K. Blockade of glucocorticoid receptors with RU486 attenuates cardiac damage and adipose tissue inflammation in a rat model of metabolic syndrome. *Hypertension Res*. 2015;38:741–750.
- De P, Roy SG, Kar D, Bandyopadhyay A. Excess of glucocorticoid induces myocardial remodeling and alteration of calcium signaling in cardiomyocytes. *J Endocrinol*. 2011;209:105–114.
- Roy SG, De P, Mukherjee D, Chander V, Konar A, Bandyopadhyay D, Bandyopadhyay A. Excess of glucocorticoid induces cardiac dysfunction via activating angiotensin II pathway. *Cell Physiol Biochem*. 2009;24:1–10.
- Lee SR, Kim HK, Youm JB, Dizon LA, Song IS, Jeong SH, Seo DY, Ko KS, Rhee BD, Kim N, Han J. Non-genomic effect of glucocorticoids on cardiovascular system. *Pflugers Arch*. 2012;464:549–559.
- He M, Yang Z, Abdellatif M, Sayed D. GTPase activating protein (Sh3 domain) binding protein 1 regulates the processing of microRNA-1 during cardiac hypertrophy. *PLoS One*. 2015;10:e0145112.
- Sayed D, He M, Yang Z, Lin L, Abdellatif M. Transcriptional regulation patterns revealed by high resolution chromatin immunoprecipitation during cardiac hypertrophy. *J Biol Chem*. 2013;288:2546–2558.
- Sayed D, Yang Z, He M, Pflieger JM, Abdellatif M. Acute targeting of general transcription factor IIB restricts cardiac hypertrophy via selective inhibition of gene transcription. *Circ Heart Fail*. 2015;8:138–148.
- Zhang Y, Liu T, Meyer CA, Eeckhoute J, Johnson DS, Bernstein BE, Nusbaum C, Myers RM, Brown M, Li W, Liu XS. Model-based analysis of ChIP-Seq (MACS). *Genome Biol*. 2008;9:R137.
- Babicki S, Arndt D, Marcu A, Liang Y, Grant JR, Maciejewski A, Wishart DS. Heatmapper: web-enabled heat mapping for all. *Nucleic Acids Res*. 2016;44:W147–W153.
- Robinson JT, Thorvaldsdottir H, Winckler W, Guttman M, Lander ES, Getz G, Mesirov JP. Integrative genomics viewer. *Nat Biotechnol*. 2011;29:24–26.
- Sayed D, Hong C, Chen IY, Lypowy J, Abdellatif M. MicroRNAs play an essential role in the development of cardiac hypertrophy. *Circ Res*. 2007;100:416–424.
- Schneider CA, Rasband WS, Eliceiri KW. NIH Image to ImageJ: 25 years of image analysis. *Nat Methods*. 2012;9:671–675.
- John S, Sabo PJ, Thurman RE, Sung MH, Biddie SC, Johnson TA, Hager GL, Stamatoyannopoulos JA. Chromatin accessibility pre-determines glucocorticoid receptor binding patterns. *Nat Genet*. 2011;43:264–268.
- Reddy TE, Pauli F, Sprouse RO, Neff NF, Newberry KM, Garabedian MJ, Myers RM. Genomic determination of the glucocorticoid response reveals unexpected mechanisms of gene regulation. *Genome Res*. 2009;19:2162–2171.
- Vockley CM, D'ippolito AM, McDowell IC, Majoros WH, Safi A, Song L, Crawford GE, Reddy TE. Direct GR binding sites potentiate clusters of TF binding across the human genome. *Cell*. 2016;166:1269–1281. e19
- Tully DB, Cidlowski JA. pBR322 contains glucocorticoid regulatory element DNA consensus sequences. *Biochem Biophys Res Commun*. 1987;144:1–10.
- Huang DW, Sherman BT, Lempicki RA. Bioinformatics enrichment tools: paths toward the comprehensive functional analysis of large gene lists. *Nucleic Acids Res*. 2009;37:1–13.
- Huang DW, Sherman BT, Lempicki RA. Systematic and integrative analysis of large gene lists using DAVID bioinformatics resources. *Nat Protoc*. 2009;4:44–57.
- Mahadeva H, Brooks G, Lodwick D, Chong NW, Samani NJ. ms1, a novel stress-responsive, muscle-specific gene that is up-regulated in the early stages of pressure overload-induced left ventricular hypertrophy. *FEBS Lett*. 2002;521:100–104.
- Subramaniam M, Hawse JR, Johnsen SA, Spelsberg TC. Role of TIEG1 in biological processes and disease states. *J Cell Biochem*. 2007;102:539–548.
- Zhao G, Jeoung NH, Burgess SC, Rosaaen-Stowe KA, Inagaki T, Latif S, Shelton JM, McAnally J, Bassel-Duby R, Harris RA, Richardson JA, Klierer SA. Overexpression of pyruvate dehydrogenase kinase 4 in heart perturbs metabolism and exacerbates calcineurin-induced cardiomyopathy. *Am J Physiol Heart Circ Physiol*. 2008;294:H936–H943.
- Aoyama T, Matsui T, Novikov M, Park J, Hemmings B, Rosenzweig A. Serum and glucocorticoid-responsive kinase-1 regulates cardiomyocyte survival and hypertrophic response. *Circulation*. 2005;111:1652–1659.
- Orth DN. Cushing's syndrome. *N Engl J Med*. 1995;332:791–803.
- Petramala L, Battisti P, Lauri G, Palleschi L, Cotesta D, Iorio M, De Toma G, Sciomer S, Letizia C. Cushing's syndrome patient who exhibited congestive heart failure. *J Endocrinol Invest*. 2007;30:525–528.
- Kamenicky P, Redheuil A, Roux C, Salenave S, Kachenoura N, Raissouni Z, Macron L, Guignat L, Jublanc C, Azarine A, Brailly S, Young J, Mousseaux E, Chanson P. Cardiac structure and function in Cushing's syndrome: a cardiac magnetic resonance imaging study. *J Clin Endocrinol Metab*. 2014;99:E2144–E2153.
- Muesan ML, Lupia M, Salvetti M, Grigoletto C, Sonino N, Boscaro M, Rosei EA, Mantero F, Fallo F. Left ventricular structural and functional characteristics in Cushing's syndrome. *J Am Coll Cardiol*. 2003;41:2275–2279.
- Iwasaki H. Reversible alterations in cardiac morphology and functions in a patient with Cushing's syndrome. *Endocrinol Diabetes Metab Case Rep*. 2014;2014:140038.
- He A, Kong SW, Ma Q, Pu WT. Co-occupancy by multiple cardiac transcription factors identifies transcriptional enhancers active in heart. *Proc Natl Acad Sci USA*. 2011;108:5632–5637.

49. Krumm A, Hickey LB, Groudine M. Promoter-proximal pausing of RNA polymerase II defines a general rate-limiting step after transcription initiation. *Genes Dev.* 1995;9:559–572.
50. Core LJ, Lis JT. Transcription regulation through promoter-proximal pausing of RNA polymerase II. *Science.* 2008;319:1791–1792.
51. Lamon S, Wallace MA, Leger B, Russell AP. Regulation of STARS and its downstream targets suggest a novel pathway involved in human skeletal muscle hypertrophy and atrophy. *J Physiol.* 2009;587:1795–1803.
52. Kuwahara K, Teg Pipes GC, McAnally J, Richardson JA, Hill JA, Bassel-Duby R, Olson EN. Modulation of adverse cardiac remodeling by STARS, a mediator of MEF2 signaling and SRF activity. *J Clin Invest.* 2007;117:1324–1334.
53. Rajamannan NM, Subramaniam M, Abraham TP, Vasile VC, Ackerman MJ, Monroe DG, Chew TL, Spelsberg TC. TGF β inducible early gene-1 (*TIEG1*) and cardiac hypertrophy: discovery and characterization of a novel signaling pathway. *J Cell Biochem.* 2007;100:315–325.
54. Bos JM, Subramaniam M, Hawse JR, Christiaans I, Rajamannan NM, Maleszewski JJ, Edwards WD, Wilde AA, Spelsberg TC, Ackerman MJ. TGF β -inducible early gene-1 (*TIEG1*) mutations in hypertrophic cardiomyopathy. *J Cell Biochem.* 2012;113:1896–1903.

SUPPLEMENTAL MATERIAL

Supplemental Tables (see Excel files)

Table S1. List of genes from RNAseq used for creating Heatmap (Figure 3).

Table S2. Genes differentially regulated after 24hrs of Dex treatment with Log₂FC values.

Table S3. Taqman gene assays used for quantitative PCR (qPCR).

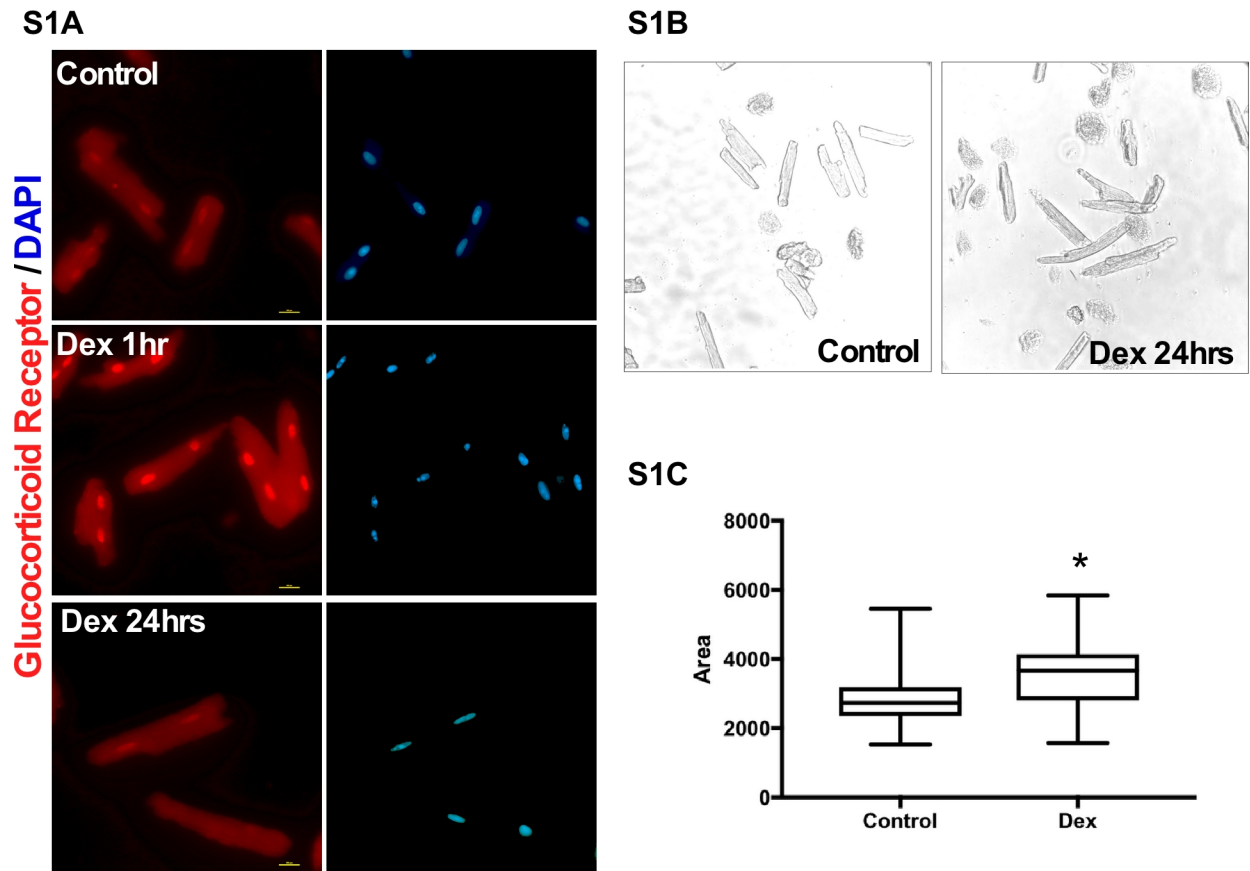


Figure S1. Isolated adult mouse ventricular cardiomyocytes treated with Dex exhibit GR nuclear translocation and cardiomyocyte hypertrophy.

A. Cardiomyocytes were treated with Ethanol (control) or Dex (100nM) for increasing time periods of 1hr or 24hrs, as indicated. Cardiomyocytes were fixed, and stained for GR (red) and DAPI (blue). Scale bar 10 μ M **B.** Isolated cultured adult mouse cardiomyocytes were treated with Ethanol or Dex for 24hrs. Phase contrast images are shown for cell size and quality of cardiomyocytes. **C.** Image J was used to measure cardiomyocyte surface area, from two independent cultures, tabulated and graphed as box plot using Prism7. * represents $p < 0.05$.

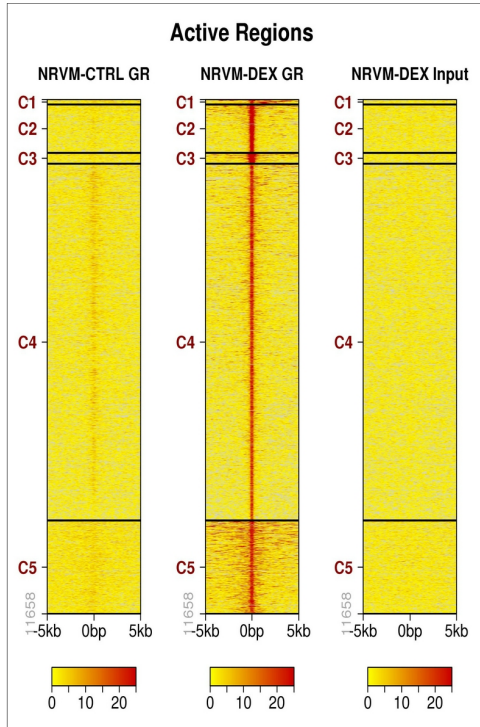
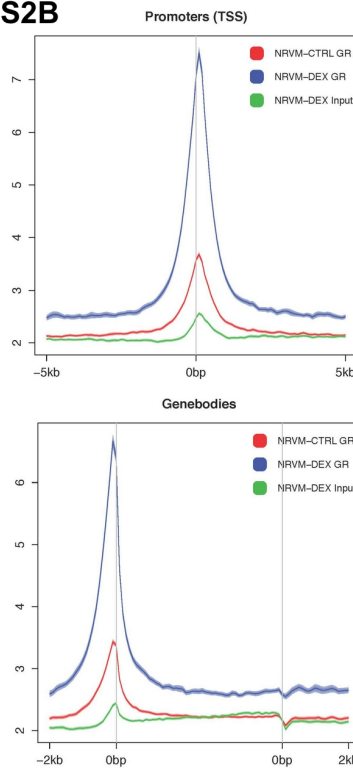
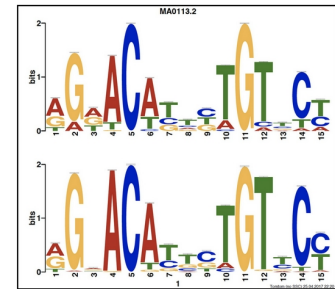
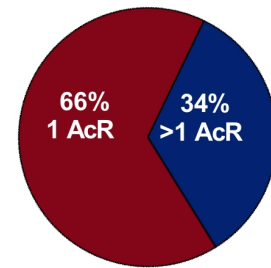
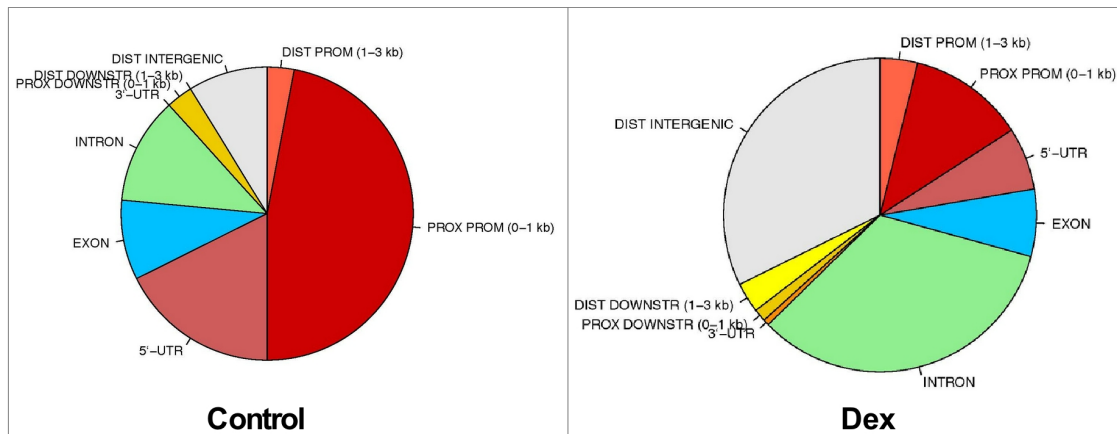
S2A**S2B****S2C****S2D****S2E**

Figure S2. GR binding and distribution across cardiac genome in neonatal cardiomyocytes treated with Dex.

A. Heatmap showing the tag distributions across active regions (values in z-axis/color, active regions in y-axis) in Control, Dex treated and Input samples. The data is presented in 5 clusters (default), C1 to C5 and sorted. **B.** Average plots of tag distributions of active regions at the transcription start site (TSS) and gene bodies are shown for Control (red), Dex treated (blue) or Input sampled (green). **C.** MEME/TOMTOM motif search identifies GRE in top 1000 peaks from GR-ChIP-seq. **D.** Pie chart showing the percent of genes associated with single active region (AcR) which represents genomic GR binding site vs. multiple Active Regions (AcR). **E.** Pie Chart showing locations of GR binding peaks relative to genomic annotations is presented as observed in Control and Dex treated samples.

S3


Genes regulated after 1hr of Dex treatment

with Gr binding						no Gr binding		
Gene.Name	# ActReg	Ave. peak value	Ave.highest ActRegs peak	RNAseq		Gene.Name	RNAseq	
		Log2Ratio Ave.	Log2Ratio Acr	Log2FC.Dex1h	Log2FC.Dex24h		Log2FC.Dex 1hr	Log2FC. Dex 24hrs
Pdk4	1	1.91	1.994	3.014	1.397	Cldn1	3.420	5.323
Arrdc3	2	2.09	2.382	2.556	0.706	Flrt3	2.112	2.090
Per1	3	4.35	4.421	2.489	2.188	Rgs1	1.926	0.335
Abra	1	4.17	4.130	2.398	1.184	Fam110c	1.435	1.198
Sox8	4	2.22	2.970	2.358	1.957	Zfp697	1.425	1.603
Aspa	1	#DIV/0!	#DIV/0!	2.251	1.506	Foxq1	1.420	1.870
Fam46b	2	4.74	5.034	2.150	3.845	Pcdh20	1.378	1.869
Klf15	3	4.38	4.622	2.129	1.987	LOC689064	1.256	1.303
Arrdc2	2	4.97	5.140	1.996	0.472	Klhl38	1.225	0.765
Sesn1	4	3.79	5.122	1.975	1.281	Zfp697	1.224	1.299
Sgk1	2	3.23	3.637	1.949	2.240	Adrb2	1.193	0.755
Cyb561	1	5.13	5.212	1.937	3.334	LOC1001348	1.184	1.157
Cpa6	2	3.46	3.920	1.757	3.218	C5ar2	1.169	2.119
Nfkbia	4	3.49	4.010	1.743	1.133	Hbb-b1	1.099	1.108
Slc10a6	1	6.17	5.151	1.639	3.247	Hba1	1.017	1.094
Rgcc	2	4.32	5.030	1.588	4.187	Gcnt1	0.975	0.438
Pkfb3	3	2.25	3.102	1.568	1.303	Hba2	0.967	1.117
Zfp189	1	4.86	4.970	1.567	0.661	Lrrc10	0.896	1.175
Errfi1	4	3.11	4.047	1.463	0.970	RGD130936z	0.873	1.227
Ptgs2	1	4.39	4.170	1.419	1.648	Lrrc10	0.871	1.095
Rasd1	2	3.12	3.660	1.331	0.850	Dgke	0.831	0.250
Klf9	5	3.70	4.977	1.323	1.569	Rnd1	-0.746	0.022
Cebpd	1	1.49	2.115	1.254	0.743	Fzd8	-0.756	-0.055
F3	3	4.62	5.401	1.222	1.363	Gja1	-0.822	-0.641
Acer2	2	3.27	4.343	1.199	2.082	Foxc2	-0.901	-0.463
Cish	4	3.53	3.950	1.106	0.268	Efnal	-1.089	-0.161
RGD1309079	2	2.10	3.265	1.104	1.550	Arc	-1.128	0.385
Slc28a2	1	2.54	2.747	1.103	2.608	G0s2	-1.129	-1.123
Relt	1	2.50	2.913	1.097	0.225	Col2a1	-1.433	-2.732
Spsb1	1	4.75	4.285	1.085	1.588	Dusp5	-1.745	-0.819
Ppp1r3b	1	1.17	1.467	0.991	-0.345			
Tob2	2	3.72	3.916	0.971	0.589			
Adamts1	1	2.25	2.713	0.935	0.896			
Dhrs3	2	2.29	3.269	0.929	0.627			
Usp53	4	1.85	3.282	0.917	1.109			
Fkbp5	6	4.13	5.079	0.904	2.686			
Tsc22d3	1	4.78	4.306	0.900	1.386			
Glul	3	2.76	3.610	0.892	1.758			
Mt2A	4	3.16	4.324	0.888	1.418			
Tsku	1	1.87	2.063	0.843	0.857			
Nt5dc3	3	3.87	4.984	0.832	1.083			
Rnf144b	3	3.37	4.363	0.831	0.500			
Cdc42ep2	3	3.42	3.976	0.812	0.414			
Cebpb	1	2.00	2.481	0.802	1.166			
Rhob	3	1.97	2.922	0.795	0.734			
RGD1304884	1	2.81	2.667	0.791	0.388			
Chst3	5	3.30	4.812	0.786	0.767			
Lpin1	3	4.13	4.475	0.771	0.336			
Mtus1	4	2.75	3.170	0.701	1.194			
Ddit4	2	1.63	3.174	0.699	0.565			
Vmp1	6	3.45	4.786	0.695	0.794			
Egr1	1	2.75	2.902	-0.715	0.038			
Ier5	2	1.31	1.793	-0.731	-0.020			
Junb	6	2.06	3.369	-0.763	0.108			
Irs1	5	2.64	4.088	-0.792	-0.186			
Irf1	2	1.62	1.922	-0.797	-0.553			
Arid5a	1	1.84	2.663	-0.871	-0.388			
Nuak2	1	3.19	2.701	-0.921	-0.016			
Klf10	2	1.56	2.118	-0.983	0.057			
Mycn	1	2.81	2.979	-0.998	-0.417			
LOC310926	2	1.73	2.681	-1.059	-1.452			
Ier3	2	2.22	2.609	-1.141	-0.516			
Hes1	5	2.28	3.329	-1.155	-0.241			
Plk2	1	1.07	1.327	-1.327	-0.757			
Lif	1	2.64	3.441	-1.360	-0.547			
Socs3	2	1.85	2.451	-1.421	-0.468			
Phlda1	1	1.78	2.252	-1.464	-0.483			
Cxcr4	1	1.42	2.121	-1.525	0.012			

Figure S3. Genes differentially regulated after 1hr of Dex treatment in neonatal cardiomyocytes.

A. Chart showing genes that are regulated after 1hr of Dex treatment with and without GR binding. Log₂ fold change (Log₂FC) is shown for GR-ChIP-seq and RNAseq data. Color scheme shows the increase (green) or decrease (red), with the color intensity corresponding to the Log₂FC values. Since some genes have multiple binding sites of GR, the average peak values are shown for gene and the active region with highest peak value.

S4 Screenshot of DAVID showing functional annotation with genes regulated after 1hr Dex


DAVID Bioinformatics Resources 6.8
Laboratory of Human Retrovirology and Immunoinformatics (LHRI)

*** Welcome to DAVID 6.8 ***
 *** If you are looking for [DAVID 6.7](#), please visit our [development site](#). ***

Functional Annotation Chart

[Help and Manual](#)

Current Gene List: 02162018 Sig Diff 1hr
Current Background: Rattus norvegicus
 92 DAVID IDs

Options

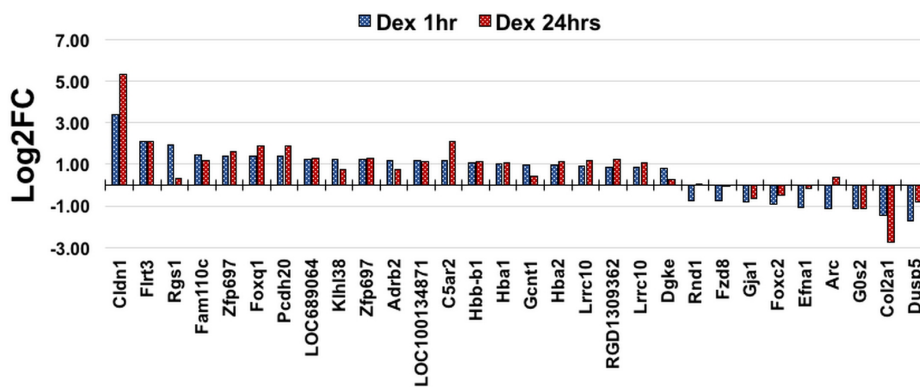
76 chart records [Download File](#)

Sublist	Category	Term	RT	Genes	Count	%	P-Value	Benjamini
<input type="checkbox"/>	GOTERM_BP_DIRECT	positive regulation of transcription from RNA polymerase II promoter	RT	<div style="width: 100%; height: 10px; background-color: #005596;"></div>	19	20.7	1.6E-6	1.5E-3
<input type="checkbox"/>	GOTERM_BP_DIRECT	positive regulation of cell death	RT	<div style="width: 20%; height: 10px; background-color: #005596;"></div>	5	5.4	1.4E-4	6.1E-2
<input type="checkbox"/>	GOTERM_BP_DIRECT	response to lipopolysaccharide	RT	<div style="width: 30%; height: 10px; background-color: #005596;"></div>	8	8.7	4.2E-4	1.2E-1
<input type="checkbox"/>	GOTERM_BP_DIRECT	regulation of gene expression	RT	<div style="width: 25%; height: 10px; background-color: #005596;"></div>	7	7.6	9.8E-4	2.1E-1
<input type="checkbox"/>	GOTERM_BP_DIRECT	cellular response to mechanical stimulus	RT	<div style="width: 20%; height: 10px; background-color: #005596;"></div>	5	5.4	1.7E-3	2.7E-1
<input type="checkbox"/>	GOTERM_BP_DIRECT	positive regulation of transcription, DNA-templated	RT	<div style="width: 100%; height: 10px; background-color: #005596;"></div>	10	10.9	1.8E-3	2.4E-1
<input type="checkbox"/>	GOTERM_BP_DIRECT	apoptotic process	RT	<div style="width: 20%; height: 10px; background-color: #005596;"></div>	8	8.7	2.0E-3	2.3E-1
<input type="checkbox"/>	GOTERM_BP_DIRECT	embryo implantation	RT	<div style="width: 10%; height: 10px; background-color: #005596;"></div>	4	4.3	2.2E-3	2.2E-1
<input type="checkbox"/>	GOTERM_BP_DIRECT	liver regeneration	RT	<div style="width: 10%; height: 10px; background-color: #005596;"></div>	4	4.3	2.4E-3	2.2E-1
<input type="checkbox"/>	GOTERM_BP_DIRECT	cellular response to insulin stimulus	RT	<div style="width: 20%; height: 10px; background-color: #005596;"></div>	5	5.4	3.0E-3	2.5E-1
<input type="checkbox"/>	GOTERM_BP_DIRECT	cellular response to peptide	RT	<div style="width: 10%; height: 10px; background-color: #005596;"></div>	3	3.3	3.8E-3	2.7E-1
<input type="checkbox"/>	GOTERM_BP_DIRECT	negative regulation of transcription, DNA-templated	RT	<div style="width: 30%; height: 10px; background-color: #005596;"></div>	9	9.8	4.2E-3	2.8E-1
<input type="checkbox"/>	GOTERM_BP_DIRECT	regulation of cell proliferation	RT	<div style="width: 20%; height: 10px; background-color: #005596;"></div>	6	6.5	5.6E-3	3.3E-1
<input type="checkbox"/>	GOTERM_BP_DIRECT	decidualization	RT	<div style="width: 10%; height: 10px; background-color: #005596;"></div>	3	3.3	9.3E-3	4.6E-1
<input type="checkbox"/>	GOTERM_BP_DIRECT	positive regulation of gene expression	RT	<div style="width: 25%; height: 10px; background-color: #005596;"></div>	7	7.6	9.3E-3	4.4E-1
<input type="checkbox"/>	GOTERM_BP_DIRECT	cellular response to drug	RT	<div style="width: 10%; height: 10px; background-color: #005596;"></div>	4	4.3	1.2E-2	5.0E-1
<input type="checkbox"/>	GOTERM_BP_DIRECT	brown fat cell differentiation	RT	<div style="width: 10%; height: 10px; background-color: #005596;"></div>	3	3.3	1.2E-2	4.8E-1
<input type="checkbox"/>	GOTERM_BP_DIRECT	negative regulation of insulin receptor signaling pathway	RT	<div style="width: 10%; height: 10px; background-color: #005596;"></div>	3	3.3	1.3E-2	5.0E-1
<input type="checkbox"/>	GOTERM_BP_DIRECT	regulation of calcium ion transport	RT	<div style="width: 10%; height: 10px; background-color: #005596;"></div>	3	3.3	1.4E-2	5.0E-1
<input type="checkbox"/>	GOTERM_BP_DIRECT	positive regulation of vascular wound healing	RT	<div style="width: 5%; height: 10px; background-color: #005596;"></div>	2	2.2	1.4E-2	4.9E-1
<input type="checkbox"/>	GOTERM_BP_DIRECT	reactive oxygen species metabolic process	RT	<div style="width: 10%; height: 10px; background-color: #005596;"></div>	3	3.3	1.5E-2	4.8E-1
<input type="checkbox"/>	GOTERM_BP_DIRECT	cellular response to peptide hormone stimulus	RT	<div style="width: 10%; height: 10px; background-color: #005596;"></div>	3	3.3	1.5E-2	4.8E-1
<input type="checkbox"/>	GOTERM_BP_DIRECT	response to insulin	RT	<div style="width: 20%; height: 10px; background-color: #005596;"></div>	4	4.3	1.5E-2	4.8E-1
<input type="checkbox"/>	GOTERM_BP_DIRECT	negative regulation of JAK-STAT cascade	RT	<div style="width: 10%; height: 10px; background-color: #005596;"></div>	3	3.3	1.8E-2	5.1E-1
<input type="checkbox"/>	GOTERM_BP_DIRECT	negative regulation of tyrosine phosphorylation of Stat1 protein	RT	<div style="width: 5%; height: 10px; background-color: #005596;"></div>	2	2.2	1.9E-2	5.3E-1
<input type="checkbox"/>	GOTERM_BP_DIRECT	circadian rhythm	RT	<div style="width: 20%; height: 10px; background-color: #005596;"></div>	4	4.3	2.1E-2	5.5E-1
<input type="checkbox"/>	GOTERM_BP_DIRECT	spongiotrophoblast differentiation	RT	<div style="width: 5%; height: 10px; background-color: #005596;"></div>	2	2.2	2.4E-2	5.8E-1
<input type="checkbox"/>	GOTERM_BP_DIRECT	response to peptide hormone	RT	<div style="width: 20%; height: 10px; background-color: #005596;"></div>	4	4.3	2.5E-2	5.8E-1
<input type="checkbox"/>	GOTERM_BP_DIRECT	cellular response to tumor necrosis factor	RT	<div style="width: 20%; height: 10px; background-color: #005596;"></div>	4	4.3	2.7E-2	6.0E-1
<input type="checkbox"/>	GOTERM_BP_DIRECT	endothelial tube morphogenesis	RT	<div style="width: 5%; height: 10px; background-color: #005596;"></div>	2	2.2	2.9E-2	6.1E-1
<input type="checkbox"/>	GOTERM_BP_DIRECT	cellular response to hypoxia	RT	<div style="width: 20%; height: 10px; background-color: #005596;"></div>	4	4.3	2.9E-2	6.0E-1
<input type="checkbox"/>	GOTERM_BP_DIRECT	cytokine-mediated signaling pathway	RT	<div style="width: 20%; height: 10px; background-color: #005596;"></div>	4	4.3	3.0E-2	5.9E-1
<input type="checkbox"/>	GOTERM_BP_DIRECT	insulin receptor signaling pathway	RT	<div style="width: 10%; height: 10px; background-color: #005596;"></div>	3	3.3	3.1E-2	6.0E-1
<input type="checkbox"/>	GOTERM_BP_DIRECT	positive regulation of protein catabolic process	RT	<div style="width: 10%; height: 10px; background-color: #005596;"></div>	3	3.3	3.3E-2	6.2E-1
<input type="checkbox"/>	GOTERM_BP_DIRECT	glomerular visceral epithelial cell differentiation	RT	<div style="width: 5%; height: 10px; background-color: #005596;"></div>	2	2.2	3.3E-2	6.1E-1
<input type="checkbox"/>	GOTERM_BP_DIRECT	regulation of auditory receptor cell differentiation	RT	<div style="width: 5%; height: 10px; background-color: #005596;"></div>	2	2.2	3.3E-2	6.1E-1
<input type="checkbox"/>	GOTERM_BP_DIRECT	response to progesterone	RT	<div style="width: 10%; height: 10px; background-color: #005596;"></div>	3	3.3	3.4E-2	6.1E-1
<input type="checkbox"/>	GOTERM_BP_DIRECT	negative regulation of cell proliferation	RT	<div style="width: 20%; height: 10px; background-color: #005596;"></div>	6	6.5	3.5E-2	6.1E-1

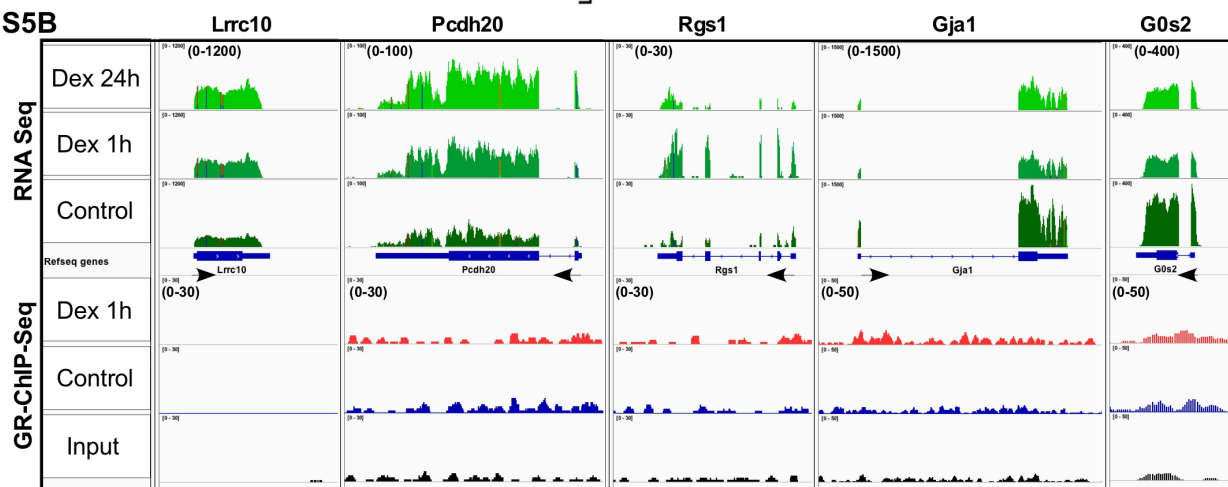
Figure S4. Functional annotation of genes regulated after 1hr of Dex in neonatal cardiomyocytes using DAVID bioinformatics resource.

Genes differentially regulated after 1hr of Dex treatment were uploaded onto the DAVID Bioinformatics resources for functional annotation. The screenshot shows the top 38 GOTERM identified by DAVID.

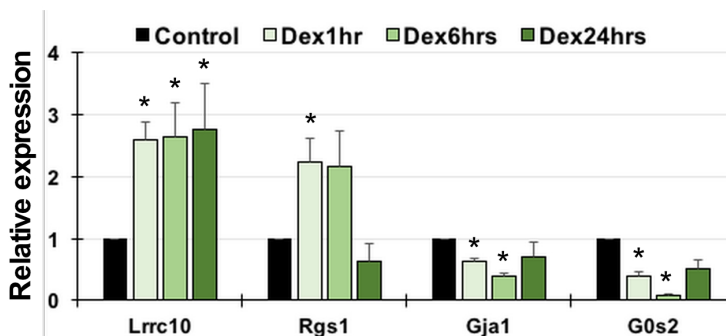
S5A



S5B



S5C



S5D

Functional Annotation of genes differentially regulated after 1 hr of Dex, but with no Gr binding

Functional Annotation Groups		Genes	P value
Embryonic heart development		2	2.70E-02
Cell-cell junction organization		2	2.80E-02
Response to dexamethasone		2	4.10E-02
Regulation of calcium ion transport		2	4.50E-02
Positive regulation of vasodilation		2	4.90E-02
Collagen fibril organization		2	4.90E-02
Heart development		3	5.00E-02
Liver regeneration		2	6.70E-02
Heart morphogenesis		2	6.90E+02
Functional Annotation Clustering (cluster 1)		Genes	P value
GOTERM_CC_Direct	integral component of plasma membrane	5	2.30E-02
GOTERM_CC_Direct	apical plasma membrane	3	5.30E-02
GOTERM_BP_Direct	G-protein coupled receptor signaling pathway	4	4.80E-01

Figure S5. Genes differentially regulated after 1hr of Dex treatment with no GR association in neonatal cardiomyocytes.

A. Graph represents genes that show significant differential regulation at 1hr and 24hrs of Dex treatment but are not associated with genomic GR binding. **B.** Integrated Genomic Viewer (IGV) screenshots of selected representative genes with aligned RNAseq and GR-ChIP-Seq data, after Dex treatment compared to control (ethanol) cardiomyocytes. Arrows indicate the direction of transcription of that genes, numbers in brackets in the Y axis indicate the values on signal tracks for GR-ChIP-Seq and RNAseq for each gene. The values were kept same within the samples for each gene. **C.** Transcript abundance of selected genes as measured by qPCR in cardiomyocytes treated with Dex for 1hr, 6hrs or 24hrs. Error bars represent SEM, * is $p < 0.05$ compared to control, $n=3$. **D.** Functional annotation of genes that showed significant differential regulation after 1hr of Dex treatment and were not associated with GR, analyzed using DAVID bioinformatics resource.

S6 Screenshot of DAVID showing Functional Annotation with genes regulated after 24hrs of Dex



*** Welcome to DAVID 6.8 ***
*** If you are looking for DAVID 6.7, please visit our development site. ***

Functional Annotation Chart

[Help and Manual](#)

Current Gene List: only 24hrs
Current Background: Rattus norvegicus
617 DAVID IDs

Options

42 chart records

Download File

Sublist	Category	Term	RT	Genes	Count	%	P-Value	Benjamini
<input type="checkbox"/>	KEGG_PATHWAY	Axon guidance	RT		20	3.2	7.6E-8	1.7E-5
<input type="checkbox"/>	KEGG_PATHWAY	Focal adhesion	RT		24	3.9	9.5E-7	1.0E-4
<input type="checkbox"/>	KEGG_PATHWAY	ECM-receptor interaction	RT		15	2.4	2.0E-6	1.5E-4
<input type="checkbox"/>	KEGG_PATHWAY	Pentose and glucuronate interconversions	RT		9	1.5	2.5E-5	1.4E-3
<input type="checkbox"/>	KEGG_PATHWAY	Metabolism of xenobiotics by cytochrome P450	RT		12	1.9	2.6E-5	1.1E-3
<input type="checkbox"/>	KEGG_PATHWAY	Ascorbate and aldarate metabolism	RT		8	1.3	2.8E-5	1.0E-3
<input type="checkbox"/>	KEGG_PATHWAY	Drug metabolism - cytochrome P450	RT		12	1.9	3.0E-5	9.4E-4
<input type="checkbox"/>	KEGG_PATHWAY	PI3K-Akt signaling pathway	RT		28	4.5	4.6E-5	1.3E-3
<input type="checkbox"/>	KEGG_PATHWAY	Chemical carcinogenesis	RT		13	2.1	6.8E-5	1.7E-3
<input type="checkbox"/>	KEGG_PATHWAY	Porphyrin and chlorophyll metabolism	RT		9	1.5	6.9E-5	1.5E-3
<input type="checkbox"/>	KEGG_PATHWAY	Retinol metabolism	RT		12	1.9	1.3E-4	2.6E-3
<input type="checkbox"/>	KEGG_PATHWAY	Complement and coagulation cascades	RT		11	1.8	1.8E-4	3.3E-3
<input type="checkbox"/>	KEGG_PATHWAY	Protein digestion and absorption	RT		12	1.9	2.4E-4	4.1E-3
<input type="checkbox"/>	KEGG_PATHWAY	Leukocyte transendothelial migration	RT		14	2.3	2.6E-4	4.1E-3
<input type="checkbox"/>	KEGG_PATHWAY	Drug metabolism - other enzymes	RT		9	1.5	6.5E-4	9.5E-3
<input type="checkbox"/>	KEGG_PATHWAY	Steroid hormone biosynthesis	RT		10	1.6	1.9E-3	2.6E-2
<input type="checkbox"/>	KEGG_PATHWAY	Renin secretion	RT		9	1.5	2.1E-3	2.8E-2
<input type="checkbox"/>	KEGG_PATHWAY	Dilated cardiomyopathy	RT		10	1.6	2.5E-3	3.0E-2
<input type="checkbox"/>	KEGG_PATHWAY	Proximal tubule bicarbonate reclamation	RT		5	0.8	6.4E-3	7.2E-2
<input type="checkbox"/>	KEGG_PATHWAY	Hypertrophic cardiomyopathy (HCM)	RT		9	1.5	6.5E-3	6.9E-2
<input type="checkbox"/>	KEGG_PATHWAY	Platelet activation	RT		12	1.9	7.3E-3	7.4E-2
<input type="checkbox"/>	KEGG_PATHWAY	Adrenergic signaling in cardiomyocytes	RT		12	1.9	1.3E-2	1.2E-1
<input type="checkbox"/>	KEGG_PATHWAY	Mineral absorption	RT		6	1.0	1.3E-2	1.2E-1
<input type="checkbox"/>	KEGG_PATHWAY	Rap1 signaling pathway	RT		15	2.4	1.8E-2	1.6E-1
<input type="checkbox"/>	KEGG_PATHWAY	Pathways in cancer	RT		23	3.7	2.1E-2	1.7E-1
<input type="checkbox"/>	KEGG_PATHWAY	Hematopoietic cell lineage	RT		8	1.3	2.2E-2	1.7E-1
<input type="checkbox"/>	KEGG_PATHWAY	Oxytocin signaling pathway	RT		12	1.9	2.4E-2	1.8E-1
<input type="checkbox"/>	KEGG_PATHWAY	Insulin secretion	RT		8	1.3	3.0E-2	2.1E-1
<input type="checkbox"/>	KEGG_PATHWAY	Arrhythmogenic right ventricular cardiomyopathy (ARVC)	RT		7	1.1	3.7E-2	2.5E-1
<input type="checkbox"/>	KEGG_PATHWAY	Bile secretion	RT		7	1.1	3.7E-2	2.5E-1
<input type="checkbox"/>	KEGG_PATHWAY	Gastric acid secretion	RT		7	1.1	4.1E-2	2.7E-1
<input type="checkbox"/>	KEGG_PATHWAY	Pertussis	RT		7	1.1	4.1E-2	2.7E-1
<input type="checkbox"/>	KEGG_PATHWAY	Calcium signaling pathway	RT		12	1.9	5.8E-2	3.5E-1
<input type="checkbox"/>	KEGG_PATHWAY	Serotonergic synapse	RT		9	1.5	6.7E-2	3.8E-1
<input type="checkbox"/>	KEGG_PATHWAY	Aldosterone synthesis and secretion	RT		7	1.1	7.2E-2	3.9E-1
<input type="checkbox"/>	KEGG_PATHWAY	Cell adhesion molecules (CAMs)	RT		11	1.8	7.7E-2	4.1E-1
<input type="checkbox"/>	KEGG_PATHWAY	Regulation of actin cytoskeleton	RT		13	2.1	7.8E-2	4.0E-1
<input type="checkbox"/>	KEGG_PATHWAY	Hippo signaling pathway	RT		10	1.6	8.6E-2	4.2E-1
<input type="checkbox"/>	KEGG_PATHWAY	Chemokine signaling pathway	RT		11	1.8	9.0E-2	4.3E-1
<input type="checkbox"/>	KEGG_PATHWAY	p53 signaling pathway	RT		6	1.0	9.6E-2	4.4E-1
<input type="checkbox"/>	KEGG_PATHWAY	Renin-angiotensin system	RT		4	0.6	9.9E-2	4.5E-1
<input type="checkbox"/>	KEGG_PATHWAY	Prion diseases	RT		4	0.6	9.9E-2	4.5E-1

Figure S6. Functional annotation of genes regulated after 24hrs of Dex in neonatal cardiomyocytes using DAVID bioinformatics resource.

Genes differentially regulated only at 24hr time point after Dex treatment compared to control cardiomyocytes were uploaded onto DAVID Bioinformatics Resources for functional annotation. The screenshot shows the 42 pathways associated with the genes as identified by KEGG pathway.

S7 Screenshot of Functional annotation of genes with GR binding and no sig diff regulation



*** Welcome to DAVID 6.8 ***
*** If you are looking for DAVID 6.7, please visit our [development site](#). ***

Functional Annotation Chart

[Help and Manual](#)

Current Gene List: **Gr binding Incremental**
Current Background: **Rattus norvegicus**
4818 DAVID IDs

Options

116 chart records

[Download File](#)

Sublist	Category	Term	RT	Genes	Count	%	P-Value	Benjamini
<input type="checkbox"/>	KEGG_PATHWAY	Protein processing in endoplasmic reticulum	RT		86	1.8	9.1E-13	2.6E-10
<input checked="" type="checkbox"/>	KEGG_PATHWAY	Spliceosome	RT		73	1.5	3.1E-12	4.4E-10
<input type="checkbox"/>	KEGG_PATHWAY	MAPK signaling pathway	RT		114	2.4	4.5E-11	4.3E-9
<input checked="" type="checkbox"/>	KEGG_PATHWAY	MicroRNAs in cancer	RT		72	1.5	2.1E-10	1.5E-8
<input type="checkbox"/>	KEGG_PATHWAY	RNA transport	RT		79	1.6	3.9E-10	2.2E-8
<input checked="" type="checkbox"/>	KEGG_PATHWAY	Thyroid hormone signaling pathway	RT		60	1.2	1.4E-9	6.9E-8
<input type="checkbox"/>	KEGG_PATHWAY	Proteoglycans in cancer	RT		84	1.7	3.4E-7	1.4E-5
<input checked="" type="checkbox"/>	KEGG_PATHWAY	Proteasome	RT		29	0.6	6.0E-7	2.1E-5
<input type="checkbox"/>	KEGG_PATHWAY	cGMP-PKG signaling pathway	RT		73	1.5	6.4E-7	2.1E-5
<input checked="" type="checkbox"/>	KEGG_PATHWAY	Pathways in cancer	RT		144	3.0	7.8E-7	2.2E-5
<input type="checkbox"/>	KEGG_PATHWAY	Non-alcoholic fatty liver disease (NAFLD)	RT		69	1.4	1.9E-6	5.0E-5
<input checked="" type="checkbox"/>	KEGG_PATHWAY	FoxO signaling pathway	RT		60	1.2	2.6E-6	6.2E-5
<input type="checkbox"/>	KEGG_PATHWAY	Ubiquitin mediated proteolysis	RT		61	1.3	3.5E-6	7.6E-5
<input checked="" type="checkbox"/>	KEGG_PATHWAY	Neurotrophin signaling pathway	RT		56	1.2	4.5E-6	9.2E-5
<input type="checkbox"/>	KEGG_PATHWAY	AMPK signaling pathway	RT		56	1.2	6.0E-6	1.1E-4
<input checked="" type="checkbox"/>	KEGG_PATHWAY	Cell cycle	RT		56	1.2	6.0E-6	1.1E-4
<input type="checkbox"/>	KEGG_PATHWAY	Alzheimer's disease	RT		74	1.5	6.1E-6	1.1E-4
<input checked="" type="checkbox"/>	KEGG_PATHWAY	Phosphatidylinositol signaling system	RT		45	0.9	8.8E-6	1.5E-4
<input type="checkbox"/>	KEGG_PATHWAY	Glucagon signaling pathway	RT		46	1.0	1.3E-5	2.0E-4
<input checked="" type="checkbox"/>	KEGG_PATHWAY	Parkinson's disease	RT		63	1.3	1.6E-5	2.4E-4
<input type="checkbox"/>	KEGG_PATHWAY	Adrenergic signaling in cardiomyocytes	RT		61	1.3	1.7E-5	2.4E-4
<input checked="" type="checkbox"/>	KEGG_PATHWAY	Metabolic pathways	RT		387	8.0	2.4E-5	3.3E-4
<input type="checkbox"/>	KEGG_PATHWAY	Oxytocin signaling pathway	RT		65	1.3	2.5E-5	3.2E-4
<input checked="" type="checkbox"/>	KEGG_PATHWAY	Huntington's disease	RT		78	1.6	3.6E-5	4.5E-4
<input type="checkbox"/>	KEGG_PATHWAY	Citrate cycle (TCA cycle)	RT		20	0.4	4.3E-5	5.1E-4
<input checked="" type="checkbox"/>	KEGG_PATHWAY	Epstein-Barr virus infection	RT		85	1.8	4.6E-5	5.3E-4
<input type="checkbox"/>	KEGG_PATHWAY	Wnt signaling pathway	RT		58	1.2	4.8E-5	5.3E-4
<input checked="" type="checkbox"/>	KEGG_PATHWAY	Endocytosis	RT		103	2.1	5.1E-5	5.4E-4
<input type="checkbox"/>	KEGG_PATHWAY	Dopaminergic synapse	RT		54	1.1	5.2E-5	5.3E-4
<input checked="" type="checkbox"/>	KEGG_PATHWAY	Prostate cancer	RT		40	0.8	7.1E-5	7.1E-4
<input type="checkbox"/>	KEGG_PATHWAY	Regulation of actin cytoskeleton	RT		81	1.7	9.7E-5	9.3E-4
<input checked="" type="checkbox"/>	KEGG_PATHWAY	Estrogen signaling pathway	RT		42	0.9	1.3E-4	1.2E-3
<input type="checkbox"/>	KEGG_PATHWAY	Renal cell carcinoma	RT		32	0.7	1.5E-4	1.3E-3
<input checked="" type="checkbox"/>	KEGG_PATHWAY	Insulin signaling pathway	RT		56	1.2	1.6E-4	1.4E-3
<input type="checkbox"/>	KEGG_PATHWAY	PI3K-Akt signaling pathway	RT		116	2.4	1.7E-4	1.4E-3
<input checked="" type="checkbox"/>	KEGG_PATHWAY	Acute myeloid leukemia	RT		28	0.6	1.7E-4	1.4E-3
<input type="checkbox"/>	KEGG_PATHWAY	Biosynthesis of antibiotics	RT		80	1.7	2.0E-4	1.6E-3
<input checked="" type="checkbox"/>	KEGG_PATHWAY	Ribosome	RT		65	1.3	3.0E-4	2.3E-3
<input type="checkbox"/>	KEGG_PATHWAY	Insulin resistance	RT		45	0.9	4.4E-4	3.3E-3
<input checked="" type="checkbox"/>	KEGG_PATHWAY	Colorectal cancer	RT		29	0.6	9.3E-4	6.8E-3
<input type="checkbox"/>	KEGG_PATHWAY	GnRH signaling pathway	RT		38	0.8	1.1E-3	7.8E-3
<input checked="" type="checkbox"/>	KEGG_PATHWAY	Hippo signaling pathway	RT		57	1.2	1.1E-3	7.7E-3
<input type="checkbox"/>	KEGG_PATHWAY	Focal adhesion	RT		74	1.5	1.2E-3	8.0E-3
<input checked="" type="checkbox"/>	KEGG_PATHWAY	Long-term potentiation	RT		29	0.6	1.2E-3	8.3E-3
<input type="checkbox"/>	KEGG_PATHWAY	Glioma	RT		29	0.6	1.2E-3	8.3E-3
<input checked="" type="checkbox"/>	KEGG_PATHWAY	Oxidative phosphorylation	RT		54	1.1	1.3E-3	8.4E-3
<input type="checkbox"/>	KEGG_PATHWAY	Chronic myeloid leukemia	RT		32	0.7	1.6E-3	1.0E-2
<input checked="" type="checkbox"/>	KEGG_PATHWAY	Circadian entrainment	RT		39	0.8	1.7E-3	1.0E-2

Figure S7. Functional annotation of genes with associated GR binding, but no significant change in transcript abundance.

Genes that were associated with GR binding but did not show significant differential change in transcript abundance on RNAseq were loaded onto DAVID Bioinformatics Resources for functional annotation. Screenshot shows top 48 pathways associated with genes as identified KEGG pathway.

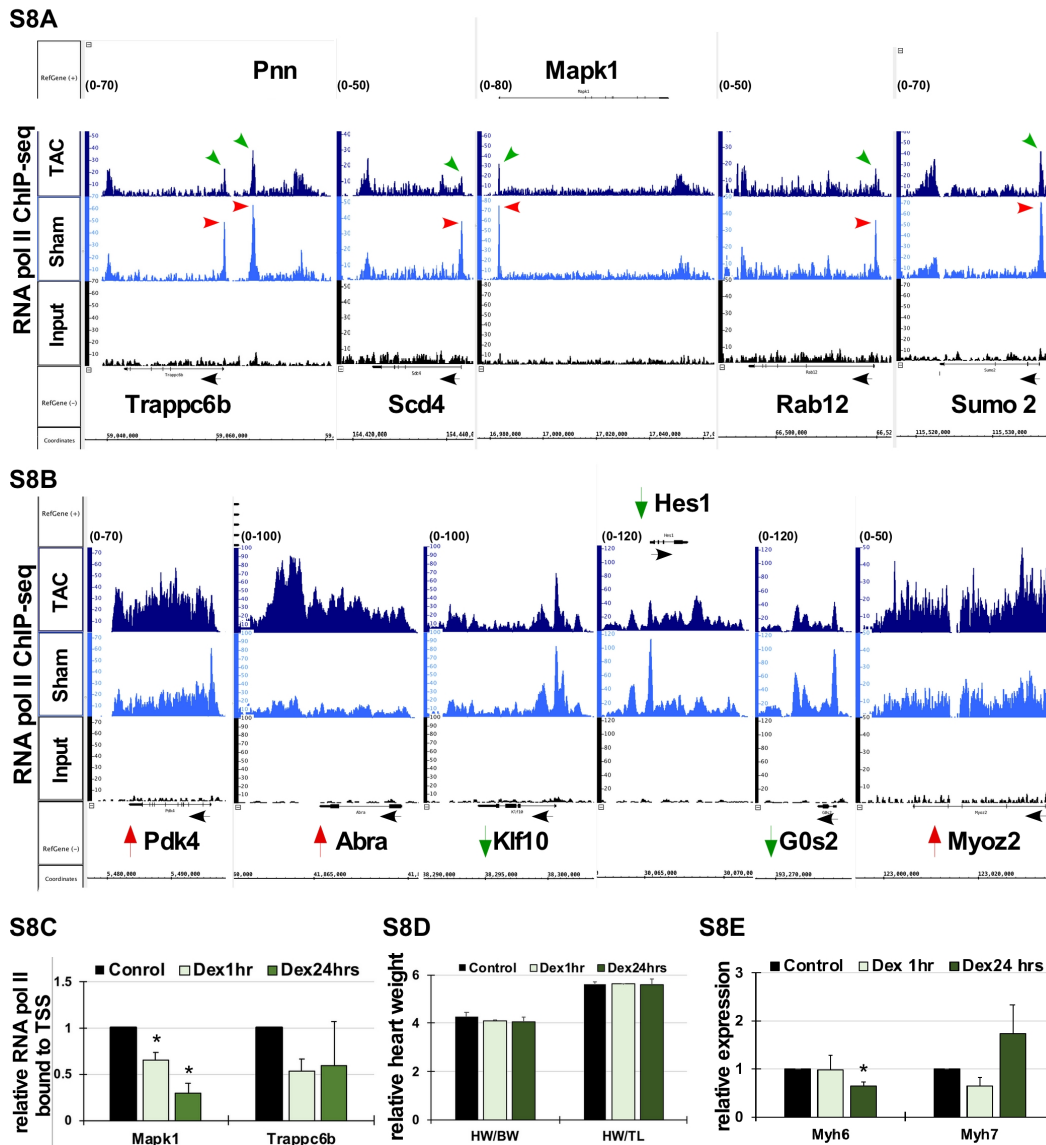
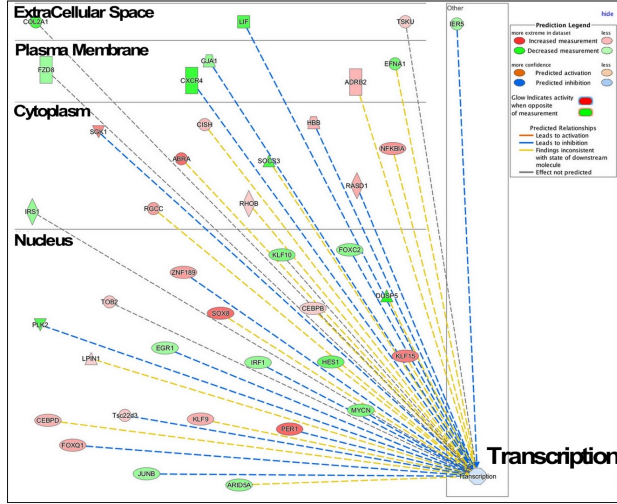
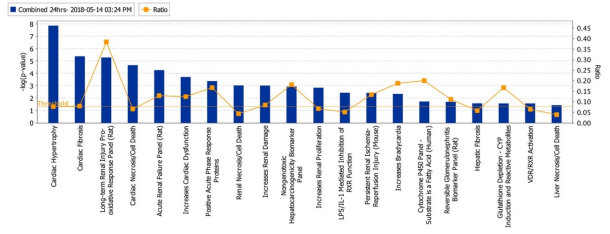


Figure S8. A. Screenshot of representative genes from RNA pol II ChIP-Seq data in mice subjected to sham or TAC operations, showing promoter paused RNA pol II peaks (red arrows) in sham hearts versus promoter clearance of these peaks (green arrow) in TAC hearts. B. RNA pol II occupancy and dynamics on genes after sham or TAC operations in mice that show significant change in transcript abundance in neonatal cardiomyocytes after Dex. These data have been described in detail in previous publication (27), and has been uploaded to GEO series GSE50637. C. RNA pol II-ChIP-qPCR was performed encompassing transcription start site (TSS) for Trappc6b and Mapk1. The graph shows relative fold enrichment of bound RNA pol II/IgG at TSS with Dex treatments for 1hr or 24hrs vs. control. Error bars represents SEM and * is $p < 0.05$. D. Graph represents heart weight (HW) to body weight (BW) or tibia length (TL) from mice injected with Dexamethasone for 1hr or 24hrs. E. Graph represents relative myh6 (alpha myosin heavy chain) and myh7 (beta myosin heavy chain) transcript abundance in mice hearts injected with Dexamethasone for 1hr or 24hrs, as indicated. Error bars for C and D indicate SEM, and * is $p < 0.05$. $n = 3-4$.

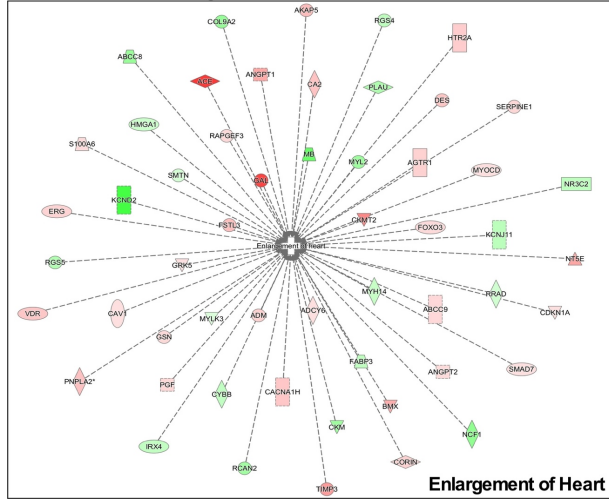
S9A Genes regulated after 1hr of Dex vs. control



S9B



S9C Genes regulated after 24hrs of Dex vs. control



S9D

Top Tox Cardiotoxicity Related Functions		
Name	P-value	# Molecules
Cardiac Enlargement	7.67E-02 - 2.05E-20	54
Heart Failure	4.72E-01 - 2.08E-17	44
Cardiac Congestive Cardiac Failure	2.62E-02 - 4.13E-13	25
Cardiac Dysfunction	2.92E-01 - 8.21E-12	28
Cardiac Infarction	1.25E-01 - 5.85E-11	30

Top Diseases and Disorders		
Name	P-value	# Molecules
Metabolic Disease	3.49E-07 - 6.11E-24	134
Cardiovascular Disease	5.83E-07 - 2.05E-20	218
Organismal Injury and Abnormalities	6.05E-07 - 2.05E-20	545
Endocrine System Disorders	5.93E-07 - 3.58E-20	188
Gastrointestinal Idisease	3.49E-07 - 3.58E-20	505

Top Physiological System Development and Function		
Name	P-value	# Molecules
Cardiovascular System Development and Function	3.63E-07 - 2.11E-30	201
Organismal Development	5.52E-07 - 7.86E-28	301
Organ Morphology	4.08E-07 - 6.32E-24	133
Skeletal and Muscular System Development and Function	3.50E-07 - 2.83E-20	136
Organismal Survival	7.20E-12 - 4.19E-19	198

Figure S9. Pathway analysis confirms Dex induction of cardiac hypertrophy –related genes. A. Genes involved in transcription network and differentially regulated after 1hr of Dex treatment vs. control cardiomyocytes are presented, as generated by IPA software, and with respect to their subcellular localization. **B.** Screenshot of IPA-Tox list from IPA software showing the genes that may be involved in toxicity function from genes regulated at 24hrs Dex vs. control. Top 20 of the list are shown in graph, where X axis represents functional list, while y axis is $-\log(p\text{-value})$. Higher the $-\log(p\text{-value})$, more significant the association. Threshold p-value is 0.05 and ratio shown is extent of overlap of data with the Tox list. Top 5 from the graph are shown in table below, with p value. **C.** Genes differentially regulated at 24hrs of Dex treatment vs. control and identified by IPA as involved in enlargement of heart is presented as a network generated by IPA software. Enlargement of heart (cardiac enlargement) was identified as the first category in cardiac hypertrophy list. **D.** Tables showing the top Tox cardiotoxicity related function, Top disease and disorders, Top physiological system development and function. The tables include the names, p-value and number of genes (#molecules) associated. Genes differentially regulated only at 24hr time point with Dex treatment vs. control were used for these analyses.